JCI The Journal of Clinical Investigation

Muscle derived interleukin-6 increases exercise capacity by signaling in osteoblasts

Subrata Chowdhury, … , Jens C. Brüning, Gerard Karsenty

J Clin Invest. 2020. https://doi.org/10.1172/JCI133572.

Research In-Press Preview Bone biology

Graphical abstract

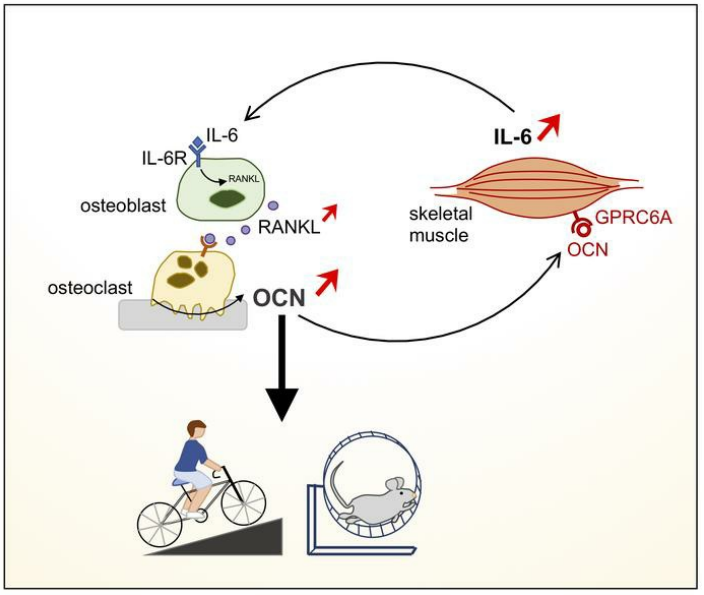

Muscle derived interleukin-6 Increases exercise capacity by signaling in osteoblasts

Subrata Chowdhury[1], Logan Schulz[1], Biagio Palmisano[1], Parminder Singh[2], Julian M. Berger[1], Vijay K. Yadav[1,2], Paula Mera[1, 3], Helga Ellingsgaard[4], Juan Hidalgo[5], Jens Brüning[6], Gerard Karsenty[1]

[1] Department of Genetics and Development, Vagelos College of Physicians and Surgeons, Columbia University, New York, NY, USA;

[2] National Institute of Immunology, New Delhi, India;

[3] Department of Biochemistry and Physiology, School of Pharmacy and Food Sciences, Institut de Biomedicina de la Universitat de Barcelona (IBUB), Universitat de Barcelona and Centro de Investigación Biomédica en Red de Fisiopatología de la Obesidad y la Nutrición (CIBEROBN), Instituto de Salud Carlos II, Spain;

[4] The Centre of Inflammation and Metabolism and the Centre for Physical Activity Research, Rigshospitalet, University of Copenhagen, 2100 Copenhagen, Denmark;

[5] Department of Cellular Biology, Physiology and Immunology Faculty of Biosciences, Universitat Autònoma de Barcelona, Spain;

[6] Max Planck Institute for Metabolism Research, Cologne, Germany.

Address correspondence to: Gerard Karsenty, Department of Genetics and Development, 701 W 168th Street, Rm. 1602A HHSC, New York, NY 10032, U.S.A; Tel: 2123056398; Email: gk2172@cumc.columbia.edu.

Keywords: Osteocalcin, Muscle-derived IL-6, IL-6R, Exercise, Osteoblast, Osteoclastogenesis, Exercise Capacity, Glucose Uptake

Abstract

Given the numerous health benefits of exercise, understanding how exercise capacity is regulated is a question of paramount importance. Circulating interleukin-6 (IL-6) levels surge during exercise and IL-6 favors exercise capacity. However, neither the cellular origin of circulating IL-6 during exercise nor the means by which this cytokine enhances exercise capacity have been formally established yet. Here we show through genetic means that the majority of circulating IL-6 detectable during exercise originates from muscle and that to increase exercise capacity, IL-6 must signal in osteoblasts to favor osteoclast differentiation and the release of bioactive osteocalcin in the general circulation. This explains why mice lacking the IL-6 receptor only in osteoblasts exhibit a deficit in exercise capacity of similar severity to the one seen in mice lacking muscle-derived IL-6 (mIL-6), and why this deficit is correctable by osteocalcin but not by IL-6. Furthermore, in agreement with the notion that IL-6 acts through osteocalcin, we demonstrate that mIL-6 promotes nutrient uptake and catabolism into myofibers during exercise in an osteocalcin-dependent manner. Lastly, we show that the crosstalk between osteocalcin and IL-6 is conserved between rodents and humans. This study

provides evidence that a muscle-bone-muscle endocrine axis is necessary to increase muscle function during exercise in rodents and humans.

Introduction

The ability to exercise, or exercise capacity, is an evolutionarily conserved physiological function of vital importance since it allows animals living in the wild to escape danger. In addition, nowadays exercise provides numerous health benefits in the general population. This explains why there is a growing interest in understanding how this physiological process is regulated (1, 2). Several cytokines have been shown to favor muscle function during exercise and as a result to increase exercise capacity (3). One of them, interleukin-6 (IL-6), sees its circulating levels surge during exercise (4-8). Since *Il6* is expressed by many cell types, this raises the question of the identity of the cell type(s) responsible for its increase in the general circulation during exercise. It has been proposed that once secreted in the general circulation, IL-6 enhances exercise capacity by promoting gluconeogenesis and lipolysis, i.e., the production of the two main nutrients for myofibers (3, 7, 9-12). However, this mechanism of action has not been verified in vivo, which leaves open the possibility that IL-6 could regulate exercise capacity through other, yet to be described, means. Those two questions are of paramount importance if we want to achieve a comprehensive understanding of how exercise capacity is regulated.

Hormones signaling in myofibers can also contribute to the increase in muscle function during exercise. In that regard, we have shown, through its injections in wild-type (WT) mice and the analysis of mice lacking its receptor only in myofibers, that the bone-

derived hormone osteocalcin is necessary and sufficient to increase muscle function during exercise in the mouse (13). Osteocalcin also promotes the rise in *Il6* expression in muscle and in circulating IL-6 levels during exercise. On the other hand, in cell culture experiments, IL-6 increased the expression in osteoblasts of *Rankl,* a gene necessary for osteoclast differentiation, a process that is required for the generation of the uncarboxylated and bioactive form of osteocalcin (osteocalcin) (13-15).

Altogether the functions of IL-6 during exercise and the relationship between osteocalcin and muscle-derived IL-6 (mIL-6) raise the following questions regarding the mechanism(s) whereby IL-6 promotes exercise capacity: To what extent does muscle contribute to the rise of circulating IL-6 during exercise? Does mIL-6 enhance exercise capacity on its own? If it does, what is its mechanism of action? Can we provide evidence that regulatory events identified in the mouse also take place in humans? The present study was conducted to address these questions.

Results

IL-6 is necessary for the increase in circulating osteocalcin levels observed in response to a training intervention in humans.

If the interplay identified in the mouse and taking place during exercise between IL-6 and osteocalcin is of real physiological significance in determining exercise capacity, it should be observed in other species including primates (13). In a first test of this contention we found that as it does in mice, a single injection of recombinant osteocalcin significantly increased circulating IL-6 levels in rats and more importantly from a clinical vantage point, in non-human primates (Figures 1A-1C).

These results led us to further expand our analysis and to measure circulating levels of bioactive osteocalcin in obese, non-diabetic human subjects that had either rested or had undergone a 12-week long aerobic training period (8). This 12-week training period consisted of endurance exercise sessions (45 minutes of biking) three times a week. We used for that purpose a novel and sensitive ELISA that specifically measures circulating uncarboxylated and bioactive human osteocalcin (osteocalcin) (13, 14). This endurance exercise training protocol resulted in a 60% increase in circulating osteocalcin levels in these individuals compared to resting individuals. Of note, this increase was sustained for at least two days after the cessation of exercise. To the best of our knowledge, this represents the first evidence that performing endurance exercise three times a week for a relatively long period of time (3-months) is enough to induce a significant increase of circulating osteocalcin levels in humans (Figure 1D).

In the third experiment we measured circulating osteocalcin levels in cohorts of exercising obese non-diabetic human individuals that received either placebo or an anti-IL-6 receptor antibody (tocilizumab) during the training period (8). We observed that in individuals that had received the anti-IL-6 receptor antibody, the increase in circulating osteocalcin levels triggered by exercise had virtually disappeared (Figure 1D). Albeit of correlative nature, this latter data is an indication that IL-6 may regulate circulating osteocalcin levels in humans as well during exercise.

Muscle derived IL-6 is needed for maximal exercise capacity

In view of the conservation of regulation between mice and humans presented above we asked to what extent does muscle contribute to the increase in circulating IL-6 levels observed during exercise and does mIL-6 actually regulate exercise capacity?

For that purpose we crossed *Il6*$^{f/f}$ mice with *Hsa-MerCreMer* mice that express the *Cre recombinase* in an inducible manner specifically in myofibers (Figure 2A) (16, 17). *Cre* expression was induced in 5-week-old mice by intraperitoneal injections of tamoxifen (i.p., 10mg/mL) 4 days in a row followed by feeding with tamoxifen-containing chow diet (1mg/20g of body weight) for 2-4 weeks prior to analysis (18). This resulted in a highly efficient deletion of *Il6* in oxidative (soleus), glycolytic (extensor digitalis or EDL), and mixed fibers muscle (gastrocnemius). In contrast, no deletion of *Il6* could be detected in the heart or any other tissues tested (Figures 2B-2C). *Il6*$_{Hsa}$*-/-* mice were obtained at the expected Mendelian ratio, had a normal life span and appeared overtly normal.

The contribution of muscle to circulating IL-6 levels during exercise was assessed by measuring its levels in male and female *Il6*$_{Hsa}$*-/-* and control mice before and after exercise (running on a treadmill at a constant speed until exhaustion or for 50 minutes) (13). We observed that while circulating IL-6 levels increased robustly in control mice after exercise, they did not in *Il6*$_{Hsa}$*-/-* mice (Figures 2D and S1A-S1B). These results indicate that the vast majority of the IL-6 molecules present in general circulation during exercise originate from muscle.

The extent to which mIL-6 contributes to exercise capacity during an endurance exercise was determined by measuring the ability of *Il6*$_{Hsa}$*-/-* and control mice to perform endurance running. Starting at 3-months of age, male and female *Il6*$_{Hsa}$*-/-* mice exhibited a significant reduction in the time and distance they run on a treadmill apparatus when compared to control littermates (Figures 2E and S1C). The defect in exercise capacity observed in *Il6*$_{Hsa}$*-/-* mice was specific to endurance exercise since grip strength was not affected by the inactivation of mIL-6 (Figures S1D-S1E). As

inferred by these results, treating WT mice with an antibody against IL-6 significantly decreased their exercise capacity (Figure 2F). The severity of the deficit in exercise capacity observed in *Il6$_{Hsa}$-/-* mice was an incentive to explore its cellular and molecular bases.

mIL-6 favors exercise capacity in part through osteocalcin

While trying to unravel how mIL-6 enhances exercise capacity, we observed that circulating osteocalcin levels did not increase in *Il6$_{Hsa}$-/-* mice after exercise as they did in control mice (Figure 3A). Moreover, *Osteocalcin*+/-;*Il6$_{Hsa}$*+/- mice exhibited a deficit in exercise capacity as severe as the one observed in *Il6$_{Hsa}$-/-* mice whereas single heterozygous mice did not and that circulating osteocalcin did not increase in *Osteocalcin*+/-;*Il6$_{Hsa}$*+/- mice during an endurance exercise. This genetic epistasis experiment indicated that osteocalcin mediates mIL-6 regulation of adaptation to exercise in the mouse, as it appears to do in humans (Figures 3B-3C).

If the aforementioned hypothesis is accurate one would expect that osteocalcin would correct at least in part the deficit in exercise capacity observed in mice lacking mIL-6. In a positive control experiment, we observed that an injection of IL-6 prior to exercise increased circulating IL-6 levels, corrected as it should the deficit in exercise capacity observed in the *Il6$_{Hsa}$-/-* mice, and restored the surge of circulating osteocalcin levels during endurance exercise (Figures 3D-3F). This IL-6 injection also corrected the deficit in exercise capacity seen in *Osteocalcin+/-; Il6$_{Hsa}$*+/- mice (Figure 3G). More importantly for our purpose, an injection of osteocalcin corrected the majority of the deficit in exercise capacity seen in *Il6$_{Hsa}$-/-* mice during endurance exercise. Of note, circulating Il-6 levels increased following these osteocalcin injections, suggesting that osteocalcin

can release IL-6 from organs other than muscle (Figures 3H-3I). These data support the notion that osteocalcin is a mediator of mIL-6 ability to enhance exercise capacity without excluding the possibility that other mediators of this action exist.

mIL-6 contributes to the maintenance of muscle mass in an osteocalcin-independent manner

In the course of this analysis we observed a second muscle phenotype in *Il6$_{Hsa}$-/-* mice. Indeed and even though *Myostatin* expression was not affected (Figure S1E), *Il6$_{Hsa}$-/-* mice demonstrate a significant decrease in the weight of oxidative muscles, e.g., the soleus, the most mobilized muscles type during an endurance exercise, in 3-month-old *Il6$_{Hsa}$-/-* mice compared to control littermates (Figure 4A). One experimental line of evidence indicates, however, that mIL-6 regulates muscle function independently or its regulation of muscle mass. Indeed, if mIL-6 and osteocalcin were in the same genetic pathway controlling exercise capacity, compound double heterozygous *Osteocalcin+/-; Il-6Hsa+/-* mice should exhibit the same deficit in exercise capacity as the one observed in *Il6$_{Hsa}$-/-* or *Osteocalcin-/-* mice whereas the single heterozygous mice would run normally. As shown in Figure 3G this is exactly what was observed. However, and as importantly, muscle mass was not decreased in any types of muscle in *Osteocalcin+/-; Il-6Hsa+/-* mice (Figure 4B). This data indicates on the one hand that the mIL-6 regulation of muscle mass and muscle function occurs through different mechanisms. On the other hand, it shows that mIL-6 regulation of muscle mass does not account for the mIL-6 regulation of exercise capacity.

To ascertain whether there are any abnormalities in Type I or Type II muscle fiber frequency in the absence of mIL6, we used two methods. First, we performed

immunohistochemistry for either the slow myosin heavy chain (Type I) or the fast myosin heavy chain (Type II) and, second, we analyzed gene expression in soleus muscle of myosin heavy chain isoform 2a (*MyHC-IIa)* and 2b (*MyHC-IIb*). In both cases there were no detectable differences in the abundance of Type I or Type II fibers in *Il6*$_{Hsa}$*-/-* and control soleus muscles (Figures 4C-4E and 4H). Likewise, an histological analysis of the soleus muscle, in 3-months-old *Il6*$_{Hsa}$*-/-* mice and control littermates and did not observe any significant difference in myofiber cross-sectional area (CSA) between *Il6*$_{Hsa}$*-/-* and control soleus muscles (Figure 4G).

IL-6 favors osteoclastogenesis by signaling in osteoblasts

Any effort to unravel the cellular pathway whereby mIL-6 enhances exercise capacity during endurance exercise must start with the identification of the cell type in which mIL-6 signals in bone. For that purpose we relied on a classical co-culture assay between osteoblasts and bone marrow-derived osteoclast progenitor cells that were obtained from mice of different genotypes (19). IL-6 exerts its biological activities through two molecules, the IL-6 receptor (IL-6R) and the glycoprotein gp130, the signal transducing partner of IL-6R (20)**.** Since gp130 contributes to the signaling of other cytokines, defining the importance of IL-6 signaling in a given cell type in vivo requires the deletion of *Il6r* in that cell type.

All co-culture experiments described below were performed in the presence of the soluble IL-6 receptor (sIL-6r) (21). When *Il6r-/-* osteoblasts were co-cultured in the presence of IL6 with *Il6r*$^{f/f}$ osteoclast progenitor cells, the number of tartrate-resistant acid phosphatase **(**TRAP) positive osteoclasts and osteoclasts containing 4 or more nuclei were both significantly reduced compared to what was observed when both

osteoblasts and osteoclast progenitor cells were derived from *Il6r*$^{f/f}$ mice or when *Il6r*$^{f/f}$ osteoblasts were co-cultured with *Il6r-/-* osteoclast progenitor cells (Figure 5A). Furthermore, expression of markers of osteoclast differentiation or function such as *Dc-stamp*, *Atp6vd02, Clcn7,* and *Acp5* was also significantly reduced in osteoclasts following co-culture of *Il6r-/-* osteoblasts with *Il6r*$^{f/f}$ osteoclast progenitor cells compared to what was observed when *Il6r*$^{f/f}$ osteoblasts were co-cultured with *Il6r*$^{f/f}$ or *Il6r-/-* osteoclasts progenitor cells (Figure 5B). We also performed co-culture experiments using *Il6r-/-* osteoblasts and *Il6r-/-* osteoclast progenitor cells in the presence of the sIL-6r. As shown in Figure 5C there was limited generation of TRAP+ multinucleated osteoclasts in this experiment. This does not exclude the formal possibility that trans IL-6 signaling contributes to osteoclastogenesis in other experimental contexts.

Lastly, we co-cultured *Il6r*$^{f/f}$ osteoblasts or osteoclast progenitor cells that had been infected beforehand with an empty adenovirus or one expressing the *Cre recombinase*. We verified in each case that infection with *Cre* achieved a deletion of *Il6r* above 65% (Figures S2A-S2B). Regardless of the presence or lack thereof of IL-6 in the culture medium, we found that when *Il6r* was deleted in osteoblasts the number of TRAP positive multinucleated osteoclasts obtained were significantly decreased compared to what was observed in co-cultures of *Il6r*$^{f/f}$ osteoclast progenitor cells and *Il6r*$^{f/f}$ osteoblasts infected with an empty adenovirus or one expressing the C*re* recombinase (Figures 5D-5E, S2C). Of note, the *RankL/Opg* ratio was significantly higher in control co-culture experiments than when the IL-6 receptor had been deleted from osteoblasts (Figure S2D). Taken together these experiments support the notion that in the

conditions of these assays, IL-6 acts primarily in cells of the osteoblast lineage to favor osteoclast differentiation.

IL-6 signaling in osteoblasts is needed to enhance exercise capacity during endurance exercise

To determine whether the ability of IL-6 signaling in osteoblasts to enhance osteoclast differentiation explains at least in part why IL-6 increases exercise capacity we crossed *Il6r*$^{f/f}$ mice with *Osteocalcin-Cre* mice that delete genes in differentiated osteoblasts after birth (Figure 6A) (22, 23). We chose this *Cre* driver mouse because we had shown earlier that mIL-6 does not influence exercise capacity in any noticeable manner before 3-months of age and therefore it seems unlikely that IL-6 functions primarily in osteoblast progenitor cells. This manipulation resulted in an efficient deletion of *Il6r* in differentiated osteoblasts but not in osteoclasts or other cell types or other tissues tested in *Il6r*$_{Osb}$*-/-* mice (Figure 6B). *Il6r*$_{Osb}$*-/-* mice were obtained at the expected Mendelian ratio, had a normal life span and appeared overtly normal.

Despite a marked increase in circulating IL-6 levels during exercise, 3- and 6-month-old *Il6r*$_{Osb}$*-/-* mice displayed a severe decrease in their ability to perform endurance exercise compared to control mice (Figures 6C-6D, S3A). In contrast, mutant mice lacking the IL-6 receptor in myofibers only ran as well as control mice (Figure 6E). The deficit in exercise capacity observed in mice lacking IL-6 signaling in osteoblasts was not caused by a decrease in muscle mass or a low bone mass since muscle mass, bone mass and markers of bone resorption at rest were all similar between *Il6r*$_{Osb}$*-/-* and control mice, despite differences in markers of bone resorptions during exercise (Figures S3B-S3D). These results indicate that IL-6 needs to signal in osteoblasts to favor exercise capacity.

Several lines of evidence indicate that the lack of secretion of bioactive osteocalcin is a major contributor to the deficit in exercise capacity of the *Il6r*$_{Osb}$*-/-* mice (Figure 6F). First, circulating osteocalcin levels did not increase in these mutant mice during endurance exercise (Figures 6C-6E). Second, compound heterozygous *Osteocalcin+/;Il6r*$_{Osb}$*+/-* mice exhibited a deficit in exercise capacity of similar severity to the one seen in *Osteocalcin-/-* or *Il6r*$_{Osb}$*-/-* mice but single heterozygous mice did not (Figure 6G) (13). Likewise, circulating osteocalcin levels did not increase in *Osteocalcin+/-;Il6r*$_{Osb}$*+/-* mice as they did in control single heterozygous littermates during exercise (Figure 6H). Third, an injection of IL-6 did not correct the deficit in exercise capacity in *Il6r*$_{Osb}$*-/-* or in *Osteocalcin+/-;Il6r*$_{Osb}$*+/-* mice even though it increased their circulating IL-6 levels (Figures 7A-7C and S3E). Fourth and conversely, an injection of osteocalcin increased exercise capacity in both *Il6r*$_{Osb}$*-/-* and *Osteocalcin+/-;Il6r*$_{Osb}$*-/-* mice (Figures 7D-7G).

mIL-6 favors glucose uptake and catabolism in myofibers during exercise through osteocalcin

In the last set of experiments we explored whether the decrease in exercise capacity caused by the absence of either muscle-derived IL-6 or IL-6 signaling in osteoblasts was secondary to a lack of substrates availability (24) or rather and as it is the case when osteocalcin signaling in myofibers is disrupted, to a decrease in substrate uptake and catabolism in muscle (13).

Glucose homeostasis assayed by glucose tolerance and insulin sensitivity tests and liver gluconeogenesis assayed by a pyruvate tolerance test, were unaffected by the post-natal deletion of *Il6* from myofibers (Figures S4A-S4E). Likewise, expression in the

liver of *Pepck* and *G6pase* that encode two key enzymes of liver gluconeogenesis was similar in *Il6$_{Hsa}$-/-*, *Il6r$_{Osb}$-/-* and control mice before and after exercise, thus indicating that gluconeogenesis is not overtly decreased in the absence of mIL-6 or of IL-6 signaling in osteoblasts (Figures S4F-S4I). The absence of any detectable decrease of substrate availability in mice lacking either mIL-6 or IL-6R in osteoblasts prompted us to test whether substrate uptake and catabolism in myofibers were decreased in the absence of mIL-6 or IL-6 signaling in osteoblasts.

Consistent with this notion we found that glucose uptake, measured by the uptake of ^{3}H-2-deoxyglucose, was decreased in oxidative muscles of both *Il6$_{Hsa}$-/-* and *Il6r$_{Osb}$-/-* mice compared to their respective control littermates (Figures 8A-8B). Moreover, expression of *Pgma1* that is necessary for glycolysis was decreased in oxidative muscles of *Il6$_{Hsa}$-/-* mice after exercise (Figure 8C). A similar decrease in glucose uptake was observed in *Osteocalcin+/-;Il6$_{Hsa}$+/-* and *Osteocalcin+/-;Il6r$_{Osb}$+/-* mice, further supporting the notion that osteocalcin mediates the positive effect of mIL-6 on glucose uptake in myofibers during exercise (Figures 8D-8E**).** To further demonstrate that this is the case we injected osteocalcin or IL-6, in *Il6$_{Hsa}$-/-, Il6r$_{Osb}$-/-*, *Osteocalcin+/-;Il6$_{Hsa}$+/-* or *Osteocalcin+/-;Il6r$_{Osb}$+/-* mice. Osteocalcin injections normalized glucose uptake in muscle in all mutant mouse strains regardless of whether they increased circulating IL-6 levels or not (Figures 8F-8I and S4J-S4M; Table 1). IL-6 injections increased circulating IL-6 levels in all mutant mouse strains and it corrected the deficit in glucose uptake only in *Il6$_{Hsa}$-/-* and *Osteocalcin+/-;Il6$_{Hsa}$+/-* mice in which circulating osteocalcin levels increased after exercise but not in *Il6r$_{Osb}$-/-* or *Osteocalcin+/-;Il6r$_{Osb}$+/-*

mice in which circulating osteocalcin levels did not increase following an IL-6 injection (Figures 8J-8K and Table 1**).**

mIL-6 favors fatty acids uptake and catabolism in myofibers during exercise through osteocalcin

Expression in white adipose tissue of *Hsl* (*Hormone sensitive lipase*) and *Atgl (Adipose triglyceride lipase)* that are necessary for lipolysis was similar in *Il6$_{Hsa}$-/-* and control mice before and after exercise (Figure S5A). Circulating levels of non-esterified fatty acids (NEFAs) and triglycerides were either normal or increased in *Il6$_{Hsa}$-/-* and *Il6r$_{Osb}$-/-* mice compared to their control littermates before and after exercise (Figures 9A-9B and S5B-S5C). Circulating glucagon and glycerol levels were also unchanged as was the expression of mitochondrial biogenesis markers in *Il6$_{Hsa}$-/-* and control mice before and after exercise (Figures S5D-S5F).

We also studied fatty acids (FAs) uptake and catabolism. As seen in mice lacking osteocalcin signaling in myofibers (13), expression of *Fatp1*, which facilitates the uptake of long-chain FAs into cells and of *Cpt1b,* which promotes their transports across the mitochondrial membrane (25), was markedly decreased in muscle of *Il6$_{Hsa}$-/-, Osteocalcin+/-;Il6$_{Hsa}$+/-* , *Il6r$_{Osb}$-/-* and *Osteocalcin+/-;Il6r$_{Osb}$+/-* mice compared to their respective controls after exercise (Figures 9C-9F). Furthermore, phosphorylation at Ser563 of HSL, the enzyme that hydrolyses intracellular triglycerides into free FAs was decreased in muscle of *Il6$_{Hsa}$-/-*, *Osteocalcin+/-;Il6$_{Hsa}$+/-*, *Il6r$_{Osb}$-/-* and *Osteocalcin+/-;Il6r$_{Osb}$+/-* mice (Figures 9G-J). Collectively these results support the notion that mIL-6 favors adaptation to exercise by promoting the production by bone of bioactive

osteocalcin that in turn increases the uptake and catabolism of nutrients, i.e., glucose and fatty acids in myofibers.

Discussion

This study was designed to address two questions related to IL-6 regulation of exercise capacity. The first one, prompted by the pleiotropic expression *of Il6*, was to determine to what extent does muscle contribute to the surge of circulating IL-6 levels during exercise. The second one was to define the cellular and molecular mechanisms used by IL-6 and/or muscle-derived IL-6 (mIL-6) to increase exercise capacity.

Addressing the first question through genetic means in the mouse established that the majority of IL-6 molecules detected in general circulation during an endurance exercise originate from myofibers. The analysis of $Il6_{Hsa}$*-/-* mice revealed several other aspects of IL-6 biology of great importance for our understanding of the regulation of exercise capacity during endurance exercise. The first one is that mIL-6 is necessary to achieve optimal exercise capacity. Second, mIL-6 is also responsible for the majority of the increase of circulating osteocalcin levels that occurs during endurance exercise. Third, the fact that an injection of osteocalcin largely rescued the deficit in exercise capacity in both $Il6_{Hsa}$*-/-* and $Il6_{Hsa}$*+/;Osteocalcin+/-* mice suggested that osteocalcin mediates at least in part the ability of IL-6 to increase exercise capacity. This assumption does not exclude the possibility that IL-6 might increase exercise capacity through additional means.

A less anticipated observation, related to muscle biology, that the analysis of $Il6_{Hsa}$*-/-* mice revealed is that mIL-6 is necessary to maintain muscle mass in adult mice. A

question this finding raised is whether this decrease in muscle explains, at least in part, the decrease in endurance exercise that the *Il6*$_{Hsa}$*-/-* mice experience. To address this question we relied on genetic epistasis, reasoning that if indeed the decrease in muscle function was secondary to the decrease in muscle mass then compound heterozygous mice lacking one allele of Osteocalcin and one allele of *Il6* in muscle should experience either both phenotypes, i.e., decrease in muscle mass and muscle function, or none of them. That *Il6*$_{Hsa}$*+/-;Osteocalcin+/-* mice exhibit the same deficit in exercise capacity as *Il6*$_{Hsa}$*-/-* mice but have a normal muscle mass indicates that the decrease in muscle function is not a consequence of the decrease in muscle mass. Of note, the decrease in muscle function during aerobic exercise also develops in *Osteocalcin-/-* mice in the face of a normal muscle mass, further indicating that muscle function is not dependent on muscle mass (13, 26). This has important implication for the treatment of the decrease in muscle function in various sarcopenic syndromes. Of note, we did not detect any overt histological changes in muscle of mice lacking mIL-6 or its receptor in osteoblasts.

Underscoring its biological importance, we note that the crosstalk between IL-6 regulation of exercise capacity and osteocalcin extends beyond the mouse since an injection of osteocalcin increases circulating IL-6 levels in non-human primates as it does in rodents (13). Furthermore, circulating osteocalcin also increased following a 12-week long training intervention in humans as it does in mice after a single bout of endurance exercise. Importantly for our purpose, this increase in circulating osteocalcin levels in humans was dependent on IL-6 signaling as is the case in the mouse. This conservation of the interplay between exercise, osteocalcin and IL-6 was a further

incentive to decipher the mechanisms whereby IL-6 regulates adaptation to exercise and the release of osteocalcin from bone.

We first established through cell-based assays that IL-6 signals primarily in osteoblasts to favor osteoclast differentiation and the release of bioactive osteocalcin. These results, obtained using genetic approaches in cell culture, are in full agreement with previous reports (19) but do not exclude the possibility that IL-6 may also act on osteoclast progenitor cells at a level we could not detect in our experimental conditions. They do not exclude either that the source of IL-6 signaling in osteoblasts might be the resorbed extracellular matrix rather than the general circulation. Regardless, these observations were an obvious incentive to analyze the consequences on exercise capacity of deleting the IL-6 receptor from osteoblasts. We used for that purpose a *Cre* driver mouse that deletes genes in differentiated osteoblasts because the deficit in exercise capacity observed in the absence of mIL-6 does not develop before three months of age, thus suggesting it is not the result of a developmental process (22). The inactivation of IL-6 signaling in differentiated osteoblasts resulted in a severe deficit in exercise capacity that develops in the face of a normal muscle mass. These results contrast with those obtained after the deletion of the IL-6 receptor in myofibers since this latter deletion does not hamper in any measurable way the ability of mice to perform an endurance exercise. They also indicate that muscle mass does not necessarily predict muscle function during exercise.

Importantly, *Il6r*$_{Osb}$*-/-* mice did not experience an increase in circulating osteocalcin during exercise and their deficit in exercise capacity was corrected by osteocalcin but not by IL-6. Taken together these results identify osteocalcin, a hormone known to

improve muscle function during exercise (13), as a major mediator of this function of IL-6 signaling in the osteoblasts. Although we did not detect in our experimental setting any measurable influence of mIL-6 in the generation of glucose and FAs, the two substrates of myofibers during exercise, we do not exclude the possibility that such a mechanism of action may also contribute to mIL-6 ability to enhance exercise capacity at a level that was not detected by the assays we used (9).

The cross-regulation between IL-6 and osteocalcin presented in earlier (13) and this study raises the question of which arm of this cross-regulation occurs first. Although this is a difficult question to address in vivo, the fact that osteocalcin acts directly on myofibers to up-regulate *Il6* expression whereas IL-6 needs to trigger a multi-step pathway involving gene expression in osteoblasts, osteoclast differentiation, and eventually release bioactive osteocalcin, suggests that the bone to muscle arm of this crosstalk is what initiates it.

The muscle to bone to muscle pathway favoring exercise capacity described here (Figure 10) complements the previously described bone to muscle pathway that is also necessary to increase exercise capacity (13). Together these two studies propose a new perspective on how exercise capacity is regulated by distinguishing between muscle mass and muscle function and by identifying bone via the hormone osteocalcin as a focal regulator of exercise capacity. They also provide credence to the notion recently proposed that bone might have evolved as a tool to escape danger (27).

Going forward two questions will need to be addressed. First, could osteocalcin signaling in myofibers be harnessed to reverse the course of sarcopenia in clinically relevant animal models of this disease? In the long run these experiments may pave the

way to harness osteocalcin signaling in muscle in order to improve muscle function in sarcopenic patients. Second, if osteocalcin emerges as a central regulator of exercise capacity it may also signal in other organs implicated in this process.

Methods and Materials

EXPERIMENTAL MODEL AND SUBJECT DETAILS

Primate studies:

Adult female rhesus monkeys (*Macaca mulatta*) weighing 7–10 kg were individually housed in standard primate cages at the large animal facility, National Institute of Immunology, New Delhi, India. All procedures were approved by the Institutional Animal Ethics Committee for the Care and Use of Primates in research (IAEC/2017/157). During the experimentation period, the temperature in the animal rooms received continuous fresh 5-µm filtered air ranged from 22–28^{0}C and 17–21^{0}C, maximum and minimum, respectively. Monkeys were injected at 1000 Hrs with recombinant human osteocalcin at the dose of 13.5 ng/g and blood samples were obtained by femoral venipuncture in Vacutainer blood collection tubes at different time points post injection. Blood was allowed to collect at room temperature, serum collected after centrifugation in aliquots and stored at -80^{0}C until analyzed.

Mouse *studies:*

Il6$^{f/f}$ and *HSA-$_{MerCreMer}$* (*HSA-$_{MCM}$*) mice (Jackson Laboratories) were on C57/BL6 genetic background. *Ocn-/-* mice were maintained on a 129-Sv genetic background. *Il6r$_{Osb}$-/-, Il6r$_{Hsa}$-/-, Il6$_{Hsa}$+/-; Ocn+/-* mice were maintained on 129-Sv/C57/BL6 mixed background. To minimize the confounding effect of a different genetic background all experiments

were performed using control littermates. All procedures involving mice were approved by CUIMC IACUC and conform to the relevant regulatory standards.

Mice genotypes were determined by PCR. For osteocalcin treatment studies *Il6*$_{Hsa}$*-/-* and *Il6r*$_{Osb}$*-/-* mice together with their controls were implanted with subcutaneous osmotic pumps (Alzet, model 1004) delivering osteocalcin (120 ng/h) for 28 days. After this period, mice were euthanized and muscles were dissected for analyses of muscle mass. Recombinant osteocalcin was purified as previously described (28).

METHODS DETAILS

Exercise

For exercise studies, all mice were trained to run on a treadmill for 4 days (17 min/day, with increasing speed from 10 to 30 cm/s, and an electric shock at 0.4 mA to trigger running). Exercise tests were performed on mice fed ad libitum at 1–6 p.m. On test day, mice were acclimated to the treadmill for 5 min, followed by 10 min running at a constant speed (17 cm/s), followed by a gradual speed increase i.p. to 30 cm/s. Mice run either until exhaustion to determine endurance capacity, or for 40 min. Mice were taken out of the grid if the number of times a mouse fell off electric grid during 1 min reaches 15 or more. For all biochemical and metabolic analyses, blood/tissues were collected and processed either at rest or at the end of a 40 min run (30 cm/s). Intraperitoneal injections of exogenous osteocalcin or IL-6 (Sigma Aldrich, I9646) were performed immediately before exercise.

Biochemistry and Molecular Biology

Glucose and insulin tolerance tests were performed as described (29). Serum osteocalcin, IL-6, glucagon levels were measured using ELISA assays. Blood glucose level was measured using an Accu-Check glucometer.

Circulatory IL-6 levels were detected using Abcam System ELISA kits in the serum of human (Abcam, ab178013), monkey (Abcam, ab119549) rat (Abcam, ab100772) and mice (Abcam, ab100712) respectively according to the manufacturer's instructions. Blood was collected from facial vein before and after exercise into tubes followed by centrifugation at 3000 X g for 10 minutes at 4^{o}C and serum aliquots were stored at -80^{o}C for further use. Mouse circulating osteocalcin levels were determined with a previously described ELISA (14). Total levels of osteocalcin and carboxylated osteocalcin were estimated using two different specific antibodies. Bioactive osteocalcin was determined by subtracting the carboxylated osteocalcin levels from total osteocalcin levels. CTX1 (Immunodiagnostic systems IDS, AC-06F1) and PiNP (Immunodiagnostic systems IDS, AC-33F1) were also measured according to manufacturer's instructions.

Circulating level of non-esterified fatty acids (NEFA), triglycerides and glycerol were determined in serum using a colorimetric triglyceride assay Kit (Biovision Inc., K622-100) and glycerol assay kit (Sigma Aldrich, MAK117) according to the manufacturer's protocol.

Gene Expression Analysis by qRT-PCR

Muscles and other organs were snap frozen in liquid nitrogen and kept at -80ºC until use. RNA was isolated using TRIZOL (Invitrogen). At the beginning RNA was incubated

with DNase I for 30 minutes at room temperature to remove any genomic DNA. DNase I-treated RNAs were converted to cDNA by using M-MLV reverse transcriptase (Thermo Fisher Scientific, 28025013) and random hexamers (Thermo Fisher Scientific, N8080127). For gene expression, 1 mg of RNA was reverse transcribed into cDNA. qPCR analyses were performed using PowerUp^{TM} SYBER green master mix (Applied Biosciences,Thermo Fisher Scientific). SYBR Green PCR conditions were 1 cycle of 50°C for 2 minutes, 1 cycle of 95°C for 10 minutes, and 40 cycles of 95°C for 15 seconds, 60°C for 60 seconds, ran by a model CFX96 Touch Real-Time PCR Detection System (Bio-Rad). Relative gene expression levels of each respective gene were calculated using the threshold cycle ($2^{-\Delta\Delta CT}$) method and normalized to *hprt*.

Protein expression analysis by Western Blot

Lysates were prepared from skeletal muscles using modified RIPA buffer (150 mM NaCl, 1 mM EDTA, 1% Triton X-100, 1% sodium deoxycholate, 0.1% SDS, and 20 mM Tris, pH 8.0) with protease inhibitors and 1 mM sodium orthovanadate with protease inhibitor cocktail (Thermo Fisher Scientific, 862209) and homogenize before quantification by BCA assay (Thermo Fisher Scientific, 23225). After adjustment of the concentration (100 µg/100 µL) in each of the samples, equal amounts of protein (20 µg) of total protein and SDS-Sample Buffer (Boston BioProducts, BP-110R), boiled for 5 minutes at 98°C, and recovered by spinning at 12,000 *g* for 5 minutes at 4°C before being loaded onto 10% or 15% SDS-PAGE gel. The gel was run for 80 minutes at 120 V in SDS-Running Buffer (Boston BioProducts, BP-177) before being transferred to a nitrocellulose membrane (Bio-Rad, 1620112) overnight for at 25 V. Blots were blocked in 5% BSA (AppliChem, A0830) in Tris-buffered saline (TBS) with 0.1% Tween for 1

hour before being incubated overnight in antibodies recognizing phospho HSL (Cell Signaling, 4137S, 1:1000), HSL (Cell Signaling, 4107, 1:1000), or GAPDH (Cell Signaling, 5174S, 1:1000). Membranes were washed with TBST buffer (137 mM NaCl, 2.7 mM KCl, 16.5 mM Tris, pH 7.4, containing 0.1% Tween-20) before being incubated with either rabbit (Santa Cruz Biotechnology, SC-2004) secondary HRP-conjugated antibodies before being imaged using ECL substrate (Bio-Rad, 170-5061) on an ImageQuant LAS-4000 (GE Healthcare, 28-9607-59AB). Band intensities were quantified using ImageJ software.

In vivo glucose uptake

A modification of a previously described method (30) was used for *in vivo* glucose uptake. Prior to exercise, mice were injected with10 µCi of ^{3}H-2-deoxyglucose (^{3}H-2DG) in 100 µl of 0.9% NaCl. Next, mice were placed on a treadmill and forced to run for 40 min at a constant speed (30 cm/s). After exercise, blood and quadriceps muscles were collected to determine ^{3}H radioactivity. ^{3}H radioactivity in blood was similar in all mice, indicating similar systemic delivery of the tracer. White and red quadriceps muscles were homogenized in 1 ml of water followed by immediate boiling for 10 min. After that, homogenates were spin at max speed for 10 min. Fifty µl of the supernatant were added to 450 µl of water and counted in 5 ml of scintillation liquid. Nine hundred µl were passed through an anion exchange column (AG 1-X8 resin, Bio-Rad) to remove 3H-2DG-6-phosphate. Column was washed with 6 ml of water and 500 µl of the eluted volume were counted in 5 ml of scintillation liquid. The difference between the total and eluted ^{3}H radioactivity represents 3H-2DG-6-phosphate accumulated in the tissue.

Recombinant Osteocalcin

Mouse uncarboxylated osteocalcin was purified from BL21 transformed with pGEX2TKmOCNas described (13, 29). Briefly, GST-osteocalcin fusion protein was produced in BL21 pLyS transformed with pGEX2TK-mOCN after induction with IPTG. Cells were collected in lysis buffer (PBS 1X, 10mM Tris pH 7.2, 2mM EDTA, 1% Triton and 1X protease and phosphatase inhibitor cocktail (Thermo Fisher Scientific, 10 78443). Following 4 freeze/thaw cycles and sonication, lysates were cleared by centrifugation. The supernatant was incubated with glutathione-sepharose 4B (GE:17075601) for 4 hours at 4°C. Following 6 washes with washing buffer (PBS 1X, 1%Triton) and with PBS 1X, osteocalcin was then cleaved out from the GST moiety by using thrombin (GE, 27-0846-01). Four fractions were collected and each of them was incubated with Benzamidine sepharose (GE, 17-5123-10) for 30 minutes at room temperature to remove thrombin.

Co-culture Osteoblast/Osteoclast

Osteoblasts were obtained from 3-5 days old mice using digestion medium containing alpha MEM, 1.5mg/ml collagenase P and 2.5% trypsin/EDTA. The cells were plated in the 6 or 24-well plate in alpha MEM with FBS (not Heat activated) and PS culture for 48-60 hours until they get confluence. For adenovirus infection 50,000-75,000 cells/well (24 well plate) were plated and infection was performed the next day. Cultures were kept in the alpha MEM with 10% FBS) till they reach confluence.

When osteoblast cultures are confluent we prepared the bone marrow cells from tibia and femur of 4-10 weeks mouse. In the culture hood extremities of each bone were cut with scissor before flushing the bone marrow into a 15ml falcon tube using a 10ml syringe connected to a 25G5/8 needle. The cell suspension was homogenized by gentle

pipetting and washed twice with alpha MEM and re-suspended in 5ml media. The cells were counted with hemacytometer and plate the cells in α-MEM medium for the desired density of 0.3 to $3X10^6$ cells/well. The medium was supplemented with serum from IL-6 *null mice (10%) and supplemented with PGE2 (10^{-6}M), Vitamin D3 (10^{-6}M) to promote RankL* and *M-CSF* expression by osteoblasts, leading to osteoclast formation. IL-6 (10ng/ml) and soluble IL6 receptor (100ng/ml) were added (21, 31). Half of the medium was changed in every 2 days being extremely careful not to aspirate the myeloid progenitor cells sitting on the osteoblasts. After co-culturing for next 5-8days, the osteoblasts layer was removed by washing 2 times with 1XPBS and then adding prewarmed 500ul digestion medium (alpha MEM+ 0.1% Collagenase +0.2% Dispase) at 37°C for 5-15 min by carefully monitoring if osteoblasts are detaching and removing the osteoblast layer completely. Once osteoblasts were detached, osteoclasts were washed again twice with PBS1X and fixed with PFA or formalin for TRAP assay or lysed in Trizol for RNA expression.

Adenovirus transduction of primary osteoblasts and bone marrow derived osteoclast precursor cells

Adenoviral vector with CMV (Cytomegalovirus) promoter (Ad5CMVEmpty) that express no protein and Adenoviral vector with CMV (Ad5CMVCRE) driving the expression of the Cre recombinase with titer $1x10^{10}$ pfu/ml were purchased from University of Iowa viral vector core. Mouse osteoblasts and bone marrow derived osteoclast precursor cells were transduced the day after they were plated into multi-well tissue culture plates with cell-culture grade PLL (Poly-L-Lysine; Sigma 0.5μl/ml). Serum-free α-MEM medium was prepared at 50% of the typical well cell culture volume (0.5ml in 12-well plate). PLL was

added just prior to addition of virus (MOI 200) and were allowed to incubated for 10min at room temperature. The virus-containing medium was used to replace the culture media and cells were returned to the incubator. After a transduction period of 12-hours, the viral medium was discarded and replaced with fresh complete medium (32).

Intraperitoneal injections

For all biochemical and metabolic analyses, blood/tissues were collected and processed either at rest or at the end of a 50 min run (30 cm/s). Intra-peritoneal injections of osteocalcin or IL-6 (Sigma) were performed immediately before exercise. To neutralize IL-6, 500**m**g of a neutralizing antibody (R&D, #MAB206) (33) was administered (i.p.) 1 hr before exercise.

Immunohistochemistry

A whole body transcardial perfusion was done with saline followed by fresh 4% PFA. The needed skeletal muscle was dissected with little force tension manipulation as possible to get the overall fusiform structure to determine axis for critical transverse embedding. The dissected muscle sample was placed in a dry weight dish for 2-3 minutes to allow for recovery from manipulation and then immersed in 20 volumes minimum of fresh 4% PFA for 16-24 hours for fixation at room temperature with agitation sufficient to move the tissue. Samples were then transfer to 1X PBS in sealed vials without any air bubble and processed for paraffin embedding.

Muscle sections (5-µm-thick) were prepared, deparaffinized with xylene, and rehydrated with a graded series of ethanol (absolute; 95%, 90%, 80%, and 70% in water). Slides were incubated in ice-cold permeabilization solution (0.1% Triton X-100

and 0.1% sodium citrate in water) and blocked in PBS containing 10% BSA and 10% normal goat serum. Sections were stained with N0Q7 antibody for MHC I slow twitch monoclonal (Sigma-Aldrich, M4276) and MY32 antibody for MHC II fast twitch monoclonal (Sigma-Aldrich, M8421), followed by 2°Ab treatment of anti-mouse IgG peroxidase staining (Sigma-Aldrich, A8924). Images were captured with a Nikon A1 confocal microscope.

Bone histology and histomorphometry

Lumbar vertebrae and tibiae from 6-month-old *Il6r*$^{f/f}$ and *Il6r*$_{Obs}^{-/-}$ mice were dissected after last exercise, fixed in 10% buffered formalin for 24 hours and dehydrated through a series of increasing ethanol concentrations. Samples were then embedded in methylmethacrylate (MMA) according to standard protocols. Von Kossa, tartrate-resistant acid phosphatase (TRAP) and toluidine blue stainings were used to measure trabecular bone volume over tissue volume (BV/TV), osteoclast and osteoblast number respectively. 6-month-old *Il6r*$^{f/f}$ and *Il6r*$_{Osb}^{-/-}$ mice were euthanized after 1 week from the last exercise. Lumbar vertebrae and tibiae were fixed in 10% buffered formalin for 24 hours and dehydrated through a series of increasing ethanol concentrations. Samples were then embedded in methylmethacrylate (MMA) according to standard protocols. 4 and 8 μm thick serial sections were cut and stained with Von Kossa, tartrate-resistant acid phosphatase (TRAP) and toluidine blue, to allow measurement of trabecular bone volume over tissue volume (BV/TV%), osteoclast and osteoblast numbers respectively. Bone histomorphometry analysis was performed on at least 30 fields at 40x magnification as described (34) using Osteomeasure Analysis system (Osteometrics).

Statistical Analysis

All values are depicted as mean ± SEM. Statistical parameters including the exact value of n, post hoc test and statistical significance are reported in every figure and figure legends. Data are estimated to be statistically significant when $p \leq 0.05$ by Student's t-test one-way or two-way ANOVA. Data were analyzed using Graph Pad Prism 7.

Study Approval

All human subjects signed a written informed consent before participating and were free to withdraw from the study at any time. The study was conducted in accordance with the guidelines for Good Clinical Practice and the Declaration of Helsinki. The study was approved by the Region Ethical Committee, Copenhagen, Denmark (H-16018062) with the registration at Clinicaltrials.gov as NCT02901496. The results have been reported in accordance with the CONSORT guidelines. All experiments involving animals were approved by the Institutional Animal Care and Use Committee of Columbia University Medical Center.

Author Contributions

S.C. and G.K. conceived of the study and designed experiments. S.C., L.S., B.P., P.S., J.M.B., V.K.Y., P.M., performed experiments. S.C. and G.K. analyzed data and wrote the manuscript.

Acknowledgement

We thank Drs. Gerald Shulman (Yale University), Patricia Ducy (Columbia University) and Mathieu Ferron (Montreal Clinical Research Institute-IRCM) for advice, reagents and reading the manuscript. This work was supported by 5R01DK104727-05 (NIDDK) (G.K.), 1R01AR073180-01A1 (NIAMS) (G.K.), Canadian Institute of Health and

Research (CIHR) Fellowship (201511MFE-359182-181537) (S.C.), Ramalingaswamy Fellowship (BT/HRD/35/02/2006) Dept. of Biotechnology, India (V.K.Y.), Ministerio de Economía y Competitividad y Fondo Europeo de Desarrollo Regional SAF2014-56546-R and RTI2018-101105-B-I00 (J.H.), TrygFonden (grants ID 101390 and ID 20045) (HE).

Declaration of Interests

The authors have declared that no conflict of interest exists.

References

1. Neufer PD, Bamman MM, Muoio DM, Bouchard C, Cooper DM, Goodpaster BH, et al. Understanding the Cellular and Molecular Mechanisms of Physical Activity-Induced Health Benefits. *Cell Metab.* 2015;22(1):4-11.
2. Zierath JR, and Wallberg-Henriksson H. Looking Ahead Perspective: Where Will the Future of Exercise Biology Take Us? *Cell Metab.* 2015;22(1):25-30.
3. Pedersen BK, and Febbraio MA. Muscles, exercise and obesity: skeletal muscle as a secretory organ. *Nat Rev Endocrinol.* 2012;8(8):457-65.
4. Ostrowski K, Rohde T, Zacho M, Asp S, and Pedersen BK. Evidence that interleukin-6 is produced in human skeletal muscle during prolonged running. *J Physiol.* 1998;508 (Pt 3):949-53.
5. Steensberg A, van Hall G, Osada T, Sacchetti M, Saltin B, and Klarlund Pedersen B. Production of interleukin-6 in contracting human skeletal muscles can account for the exercise-induced increase in plasma interleukin-6. *J Physiol.* 2000;529 Pt 1:237-42.
6. Pedersen BK, Steensberg A, Fischer C, Keller C, Keller P, Plomgaard P, et al. Searching for the exercise factor: is IL-6 a candidate? *J Muscle Res Cell Motil.* 2003;24(2-3):113-9.
7. Lang Lehrskov L, Lyngbaek MP, Soederlund L, Legaard GE, Ehses JA, Heywood SE, et al. Interleukin-6 Delays Gastric Emptying in Humans with Direct Effects on Glycemic Control. *Cell Metab.* 2018;27(6):1201-11 e3.
8. Wedell-Neergaard AS, Lang Lehrskov L, Christensen RH, Legaard GE, Dorph E, Larsen MK, et al. Exercise-Induced Changes in Visceral Adipose Tissue Mass Are Regulated by IL-6 Signaling: A Randomized Controlled Trial. *Cell Metab.* 2019;29(4):844-55 e3.
9. Febbraio MA, Hiscock N, Sacchetti M, Fischer CP, and Pedersen BK. Interleukin-6 is a novel factor mediating glucose homeostasis during skeletal muscle contraction. *Diabetes.* 2004;53(7):1643-8.
10. van Hall G, Steensberg A, Sacchetti M, Fischer C, Keller C, Schjerling P, et al. Interleukin-6 stimulates lipolysis and fat oxidation in humans. *J Clin Endocrinol Metab.* 2003;88(7):3005-10.
11. Catoire M, and Kersten S. The search for exercise factors in humans. *FASEB J.* 2015;29(5):1615-28.
12. Hawley JA, Hargreaves M, Joyner MJ, and Zierath JR. Integrative biology of exercise. *Cell.* 2014;159(4):738-49.

13. Mera P, Laue K, Ferron M, Confavreux C, Wei J, Galan-Diez M, et al. Osteocalcin Signaling in Myofibers Is Necessary and Sufficient for Optimum Adaptation to Exercise. *Cell Metab.* 2016;23(6):1078-92.
14. Ferron M, Wei J, Yoshizawa T, Del Fattore A, DePinho RA, Teti A, et al. Insulin signaling in osteoblasts integrates bone remodeling and energy metabolism. *Cell.* 2010;142(2):296-308.
15. Johnson RW, Brennan HJ, Vrahnas C, Poulton IJ, McGregor NE, Standal T, et al. The primary function of gp130 signaling in osteoblasts is to maintain bone formation and strength, rather than promote osteoclast formation. *J Bone Miner Res.* 2014;29(6):1492-505.
16. McCarthy JJ, Srikuea R, Kirby TJ, Peterson CA, and Esser KA. Correction: Inducible Cre transgenic mouse strain for skeletal muscle-specific gene targeting. *Skelet Muscle.* 2012;2(1):22.
17. Miniou P, Tiziano D, Frugier T, Roblot N, Le Meur M, and Melki J. Gene targeting restricted to mouse striated muscle lineage. *Nucleic Acids Res.* 1999;27(19):e27.
18. von Maltzahn J, Jones AE, Parks RJ, and Rudnicki MA. Pax7 is critical for the normal function of satellite cells in adult skeletal muscle. *Proc Natl Acad Sci U S A.* 2013;110(41):16474-9.
19. Suda T, Takahashi N, and Martin TJ. Modulation of osteoclast differentiation. *Endocr Rev.* 1992;13(1):66-80.
20. Mihara M, Hashizume M, Yoshida H, Suzuki M, and Shiina M. IL-6/IL-6 receptor system and its role in physiological and pathological conditions. *Clin Sci (Lond).* 2012;122(4):143-59.
21. McGregor NE, Murat M, Elango J, Poulton IJ, Walker EC, Crimeen-Irwin B, et al. IL-6 exhibits both cis- and trans-signaling in osteocytes and osteoblasts, but only trans-signaling promotes bone formation and osteoclastogenesis. *J Biol Chem.* 2019;294(19):7850-63.
22. Zhang M, Xuan S, Bouxsein ML, von Stechow D, Akeno N, Faugere MC, et al. Osteoblast-specific knockout of the insulin-like growth factor (IGF) receptor gene reveals an essential role of IGF signaling in bone matrix mineralization. *J Biol Chem.* 2002;277(46):44005-12.
23. Wunderlich FT, Strohle P, Konner AC, Gruber S, Tovar S, Bronneke HS, et al. Interleukin-6 signaling in liver-parenchymal cells suppresses hepatic inflammation and improves systemic insulin action. *Cell Metab.* 2010;12(3):237-49.
24. Perry RJ, Camporez JG, Kursawe R, Titchenell PM, Zhang D, Perry CJ, et al. Hepatic acetyl CoA links adipose tissue inflammation to hepatic insulin resistance and type 2 diabetes. *Cell.* 2015;160(4):745-58.
25. Stahl A, Gimeno RE, Tartaglia LA, and Lodish HF. Fatty acid transport proteins: a current view of a growing family. *Trends Endocrinol Metab.* 2001;12(6):266-73.
26. Mera P, Laue K, Wei J, Berger JM, and Karsenty G. Corrigendum to "Osteocalcin is necessary and sufficient to maintain muscle mass in older mice" [Mol Metabol 5 (2017) 1042-1047]. *Mol Metab.* 2017;6(8):941.
27. Berger JM, Singh P, Khrimian L, Morgan DA, Chowdhury S, Arteaga-Solis E, et al. Mediation of the Acute Stress Response by the Skeleton. *Cell Metab.* 2019;30(5):890-902 e8.
28. Oury F, Khrimian L, Denny CA, Gardin A, Chamouni A, Goeden N, et al. Maternal and offspring pools of osteocalcin influence brain development and functions. *Cell.* 2013;155(1):228-41.
29. Lee NK, Sowa H, Hinoi E, Ferron M, Ahn JD, Confavreux C, et al. Endocrine regulation of energy metabolism by the skeleton. *Cell.* 2007;130(3):456-69.
30. Howlett KF, Andrikopoulos S, Proietto J, and Hargreaves M. Exercise-induced muscle glucose uptake in mice with graded, muscle-specific GLUT-4 deletion. *Physiol Rep.* 2013;1(3):e00065.
31. Tamura T, Udagawa N, Takahashi N, Miyaura C, Tanaka S, Yamada Y, et al. Soluble interleukin-6 receptor triggers osteoclast formation by interleukin 6. *Proc Natl Acad Sci U S A.* 1993;90(24):11924-8.

32. Buo AM, Williams MS, Kerr JP, and Stains JP. A cost-effective method to enhance adenoviral transduction of primary murine osteoblasts and bone marrow stromal cells. *Bone Res.* 2016;4:16021.
33. Pedersen L, Idorn M, Olofsson GH, Lauenborg B, Nookaew I, Hansen RH, et al. Voluntary Running Suppresses Tumor Growth through Epinephrine- and IL-6-Dependent NK Cell Mobilization and Redistribution. *Cell Metab.* 2016;23(3):554-62.
34. Yadav VK, Ryu JH, Suda N, Tanaka KF, Gingrich JA, Schutz G, et al. Lrp5 controls bone formation by inhibiting serotonin synthesis in the duodenum. *Cell.* 2008;135(5):825-37.

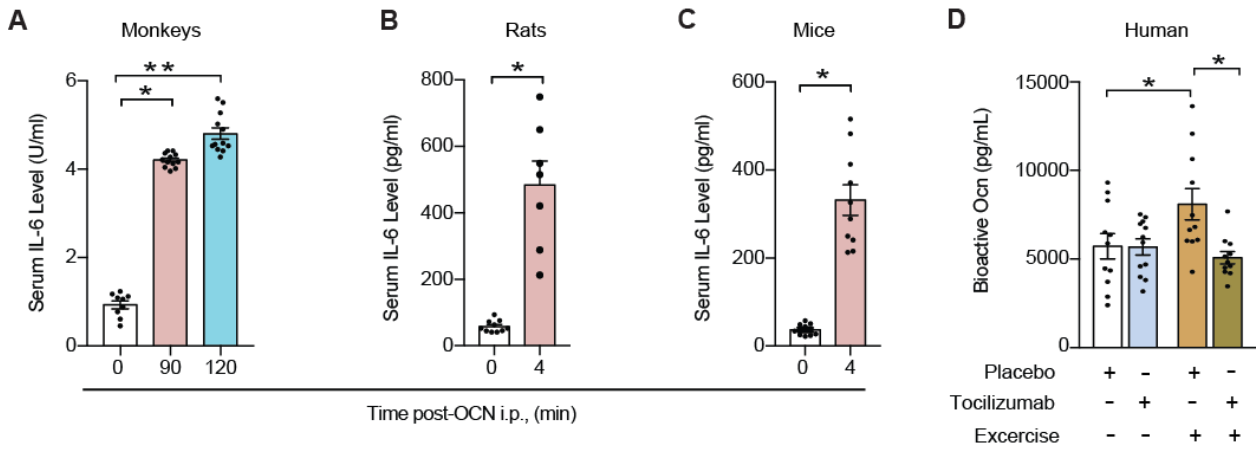

Figure 1: IL-6 is necessary for the increase in circulating osteocalcin levels observed in response to a training intervention in humans.

(**A-C**) Circulating IL-6 levels in (**A**) rhesus monkeys (14±0.8 year-old), (**B**) rats (4 month-old), (**C**) Mice (3 month-old) treated with vehicle or osteocalcin (Ocn) (13.5ng/g for monkeys, 30ng/g for rats and 30ng/g for mice). Data represent means ± SEM. n=12 per treatment. Statistical analyses were conducted using 1-way ANOVA followed by Tukey's post hoc test (A) or 2-tailed unpaired t test (B-C). (**D**) Circulating uncarboxylated and bioactive Ocn levels in obese, non-diabetic subjects treated with either placebo or a neutralizing antibody against the IL-6 receptor in combination with or without intensive endurance exercise for 45 min three times a week for 12 consecutive weeks. n=11 per group except no exercise with Tocilizumab group n=12. Statistical analyses were conducted using 1-way ANOVA followed by Holm-Sidak's post hoc test. Results represent the mean ± SEM. *P <0.05, **P <0.01.

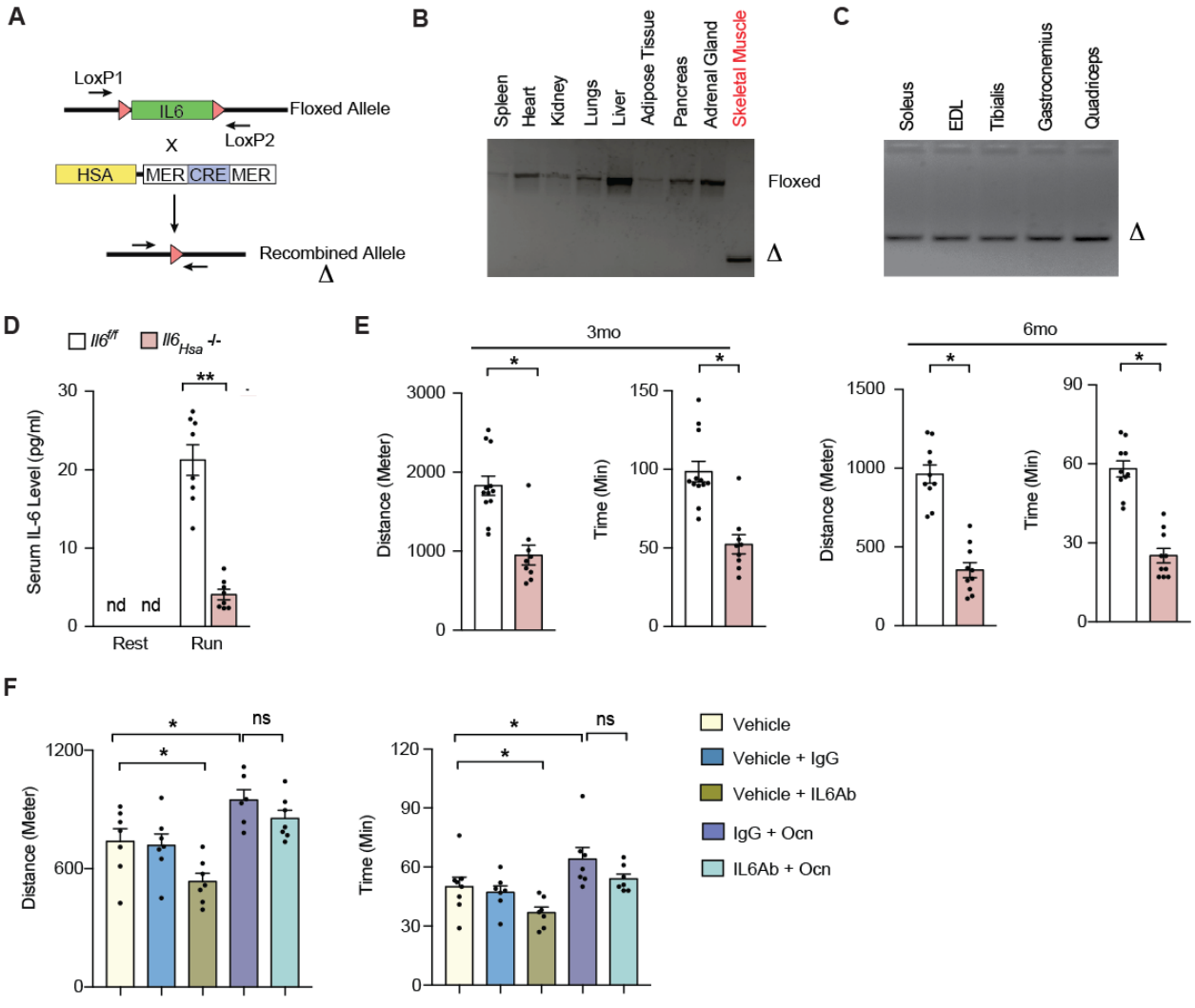
A
LoxP1
IL6
Floxed Allele
X
LoxP2
HSA
MER CRE MER
Recombined Allele
Δ
B
Spleen
Heart
Kidney
Lungs
Liver
Adipose Tissue
Pancreas
Adrenal Gland
Skeletal Muscle
Floxed
Δ
C
Soleus
EDL
Tibialis
Gastrocnemius
Quadriceps
Δ
D
Il6f/f
Il6Hsa -/-
Serum IL-6 Level (pg/ml)
nd nd
Rest
Run
E
3mo
6mo
Distance (Meter)
Time (Min)
F
Distance (Meter)
Time (Min)
ns
Vehicle
Vehicle + IgG
Vehicle + IL6Ab
IgG + Ocn
IL6Ab + Ocn

1

2

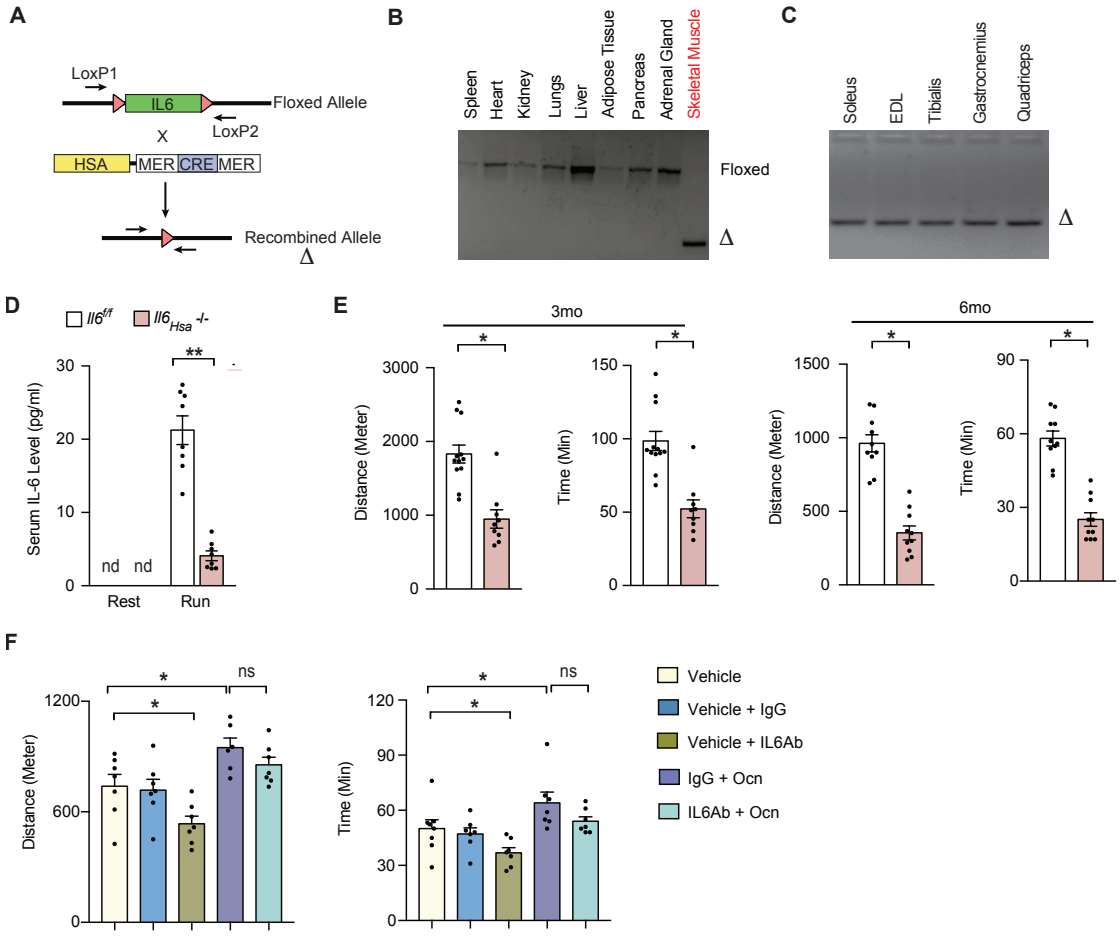
A
LoxP1
IL6
Floxed Allele
X
LoxP2
HSA
MER CRE MER
Recombined Allele
Δ
B
Spleen
Heart
Kidney
Lungs
Liver
Adipose Tissue
Pancreas
Adrenal Gland
Skeletal Muscle
Floxed
Δ
C
Soleus
EDL
Tibialis
Gastrocnemius
Quadriceps
Δ
D
Il6f/f
Il6Hsa -/-
Serum IL-6 Level (pg/ml)
nd nd
Rest
Run
E
3mo
6mo
Distance (Meter)
Time (Min)
F
Distance (Meter)
Time (Min)
ns
Vehicle
Vehicle + IgG
Vehicle + IL6Ab
IgG + Ocn
IL6Ab + Ocn

Figure 2: Muscle derived IL-6 is needed for maximal exercise capacity.

(**A**) The promoter of the human α-skeletal actin (*HSA*) gene drives expression of the *MerCreMer (MCM)* gene, which harbors a mutated estrogen receptor (Mer) ligand-binding domain on each end of the *Cre recombinase*. After crossing with $Il6^{f/f}$ mice and treatment with tamoxifen a Cre-mediated recombination event results in the deletion of the *Il6* gene. (**B**) Detection of *Il6* deletion by PCR on genomic DNA isolated from various tissues of $Il6_{Hsa}$-/- mice. **(C)** Detection of *Il6* deletion by PCR on genomic DNA isolated from various skeletal muscles of $Il6_{Hsa}$-/- mice. (**D**) Circulating IL-6 levels in 3-month-old male $Il6^{f/f}$ and $Il6_{Hsa}$-/- mice at rest and after exercise. n=8 per group (**E**) Performance during an endurance run of 3 and 6-month-old $Il6^{f/f}$ and $Il6_{Hsa}$-/- female mice. (**F**) Performance during an endurance test (running on a treadmill at 30 cm/s until exhaustion) of 8-month-old mice treated with vehicle or osteocalcin (500ng/g) and an antibody against IL-6 or a control IgG, n=7 per group. Results represent the mean± SEM. Data were analyzed with 2-tailed unpaired t test **(**D, E**)** and one-way ANOVA followed by Tukey's post hoc test (F) ***P* <0.05, ** *P* <0.01

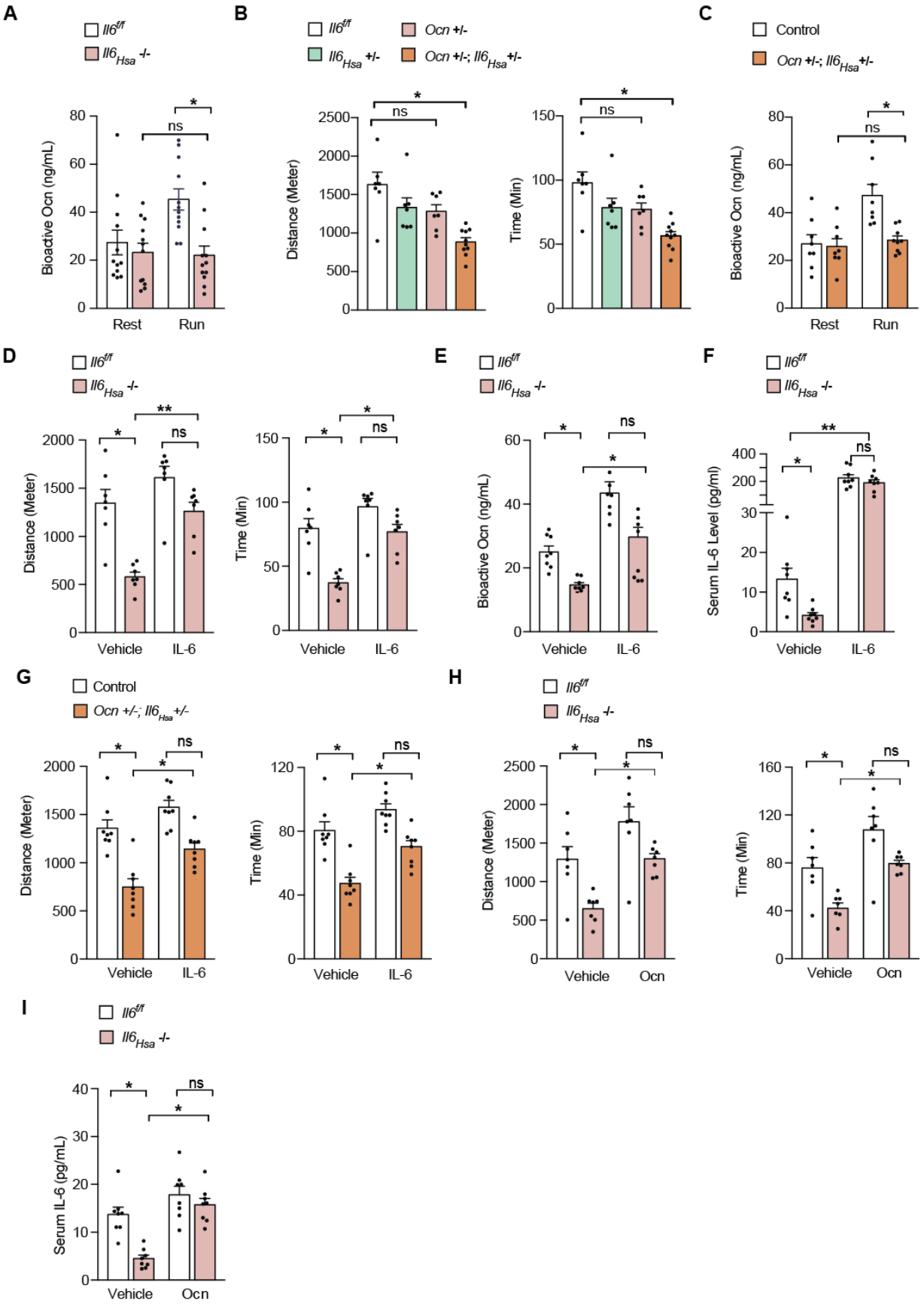
A
Il6f/f
Il6Hsa -/-
Bioactive Ocn (ng/mL)
Rest
Run
B
Il6f/f
Il6Hsa +/-
Ocn +/-
Ocn +/-; Il6Hsa+/-
Distance (Meter)
Time (Min)
C
Control
Ocn +/-; Il6Hsa+/-
Bioactive Ocn (ng/mL)
D
Distance (Meter)
Time (Min)
Vehicle
IL-6
E
Bioactive Ocn (ng/mL)
F
Serum IL-6 Level (pg/ml)
G
Distance (Meter)
Time (Min)
H
Distance (Meter)
Time (Min)
Ocn
I
Serum IL-6 (pg/mL)
ns

1

Figure 3: mIL-6 favors exercise capacity in part through osteocalcin

(**A**) Circulating bioactive Ocn (Ocn) levels in 3-month-old *Il6$^{f/f}$* and *Il6$_{Hsa}$-/-* mice at rest and after exercise, n=12. (**B**) Performance during an endurance run of 3-month-old *Osteocalcin+/-;Il6$_{Hsa}$+/-* and control *(Il6$_{Hsa}$+/-, Osteocalcin+/-* and WT) mice, n=8-12. (**C**) Circulating Ocn levels in 3-month-old control (*Il6$^{f/f}$*, *Osteocalcin+/- a*nd WT mice) and *Osteocalcin+/-;Il6$_{Hsa}$+/-* mice at rest and after exercise, n=8. (**D**) Performance during an endurance run of 3-month-old *Il6$^{f/f}$* and *Il6$_{Hsa}$-/-* mice after an i.p. injection of IL-6. (3ng/g), n=8 (**E**) Circulating Ocn levels during an endurance run in 3-month-old *Il6$^{f/f}$* and *Il6$_{Hsa}$-/-* mice after an i.p. injection of IL-6 (3ng/g), n=8. (**F**) Circulating IL-6 levels during an endurance run in 3-month-old *Il6$^{f/f}$* and *Il6$_{Hsa}$-/-* mice after an i.p. injection of IL-6 (3ng/g), n=8. (**G**) Performance during an endurance run of 3-month-old control (*Il6$^{f/f}$*, *Osteocalcin+/- a*nd WT mice) and *Osteocalcin+/-; Il6$_{Hsa}$+/-* mice after an i.p. injection of IL-6 (3ng/g), n=8. (**H**) Performance during an endurance run of 3-month-old *Il6$^{f/f}$* and *Il6$_{Hsa}$-/-* mice after an i.p. Ocn injection (120ng/g), n=7. (I) Circulating IL-6 levels during an endurance run in 3-month-old *Il6$^{f/f}$* and *Il6$_{Hsa}$-/-* mice after an i.p. injection of osteocalcin (120ng/g), n=8. These experiments are representative of 3 independent experiments. Data shown were analyzed by one-way ANOVA followed by Tukey's post hoc test. Results represent the mean± SEM. ***P* <0.05; ****P* <0.01.

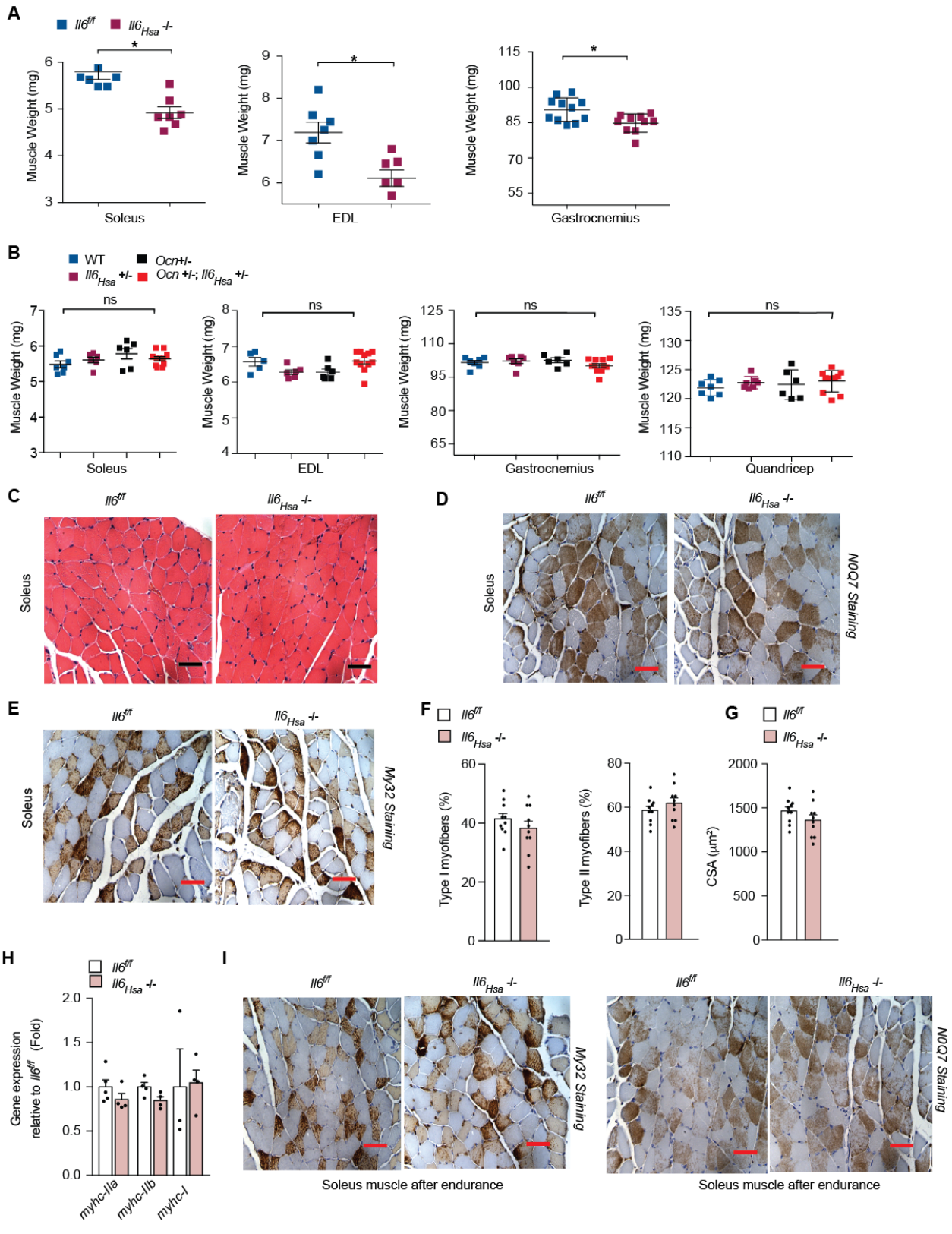
A
Il6f/f
Il6Hsa -/-
Muscle Weight (mg)
Soleus
EDL
Gastrocnemius
B
WT
Ocn+/-
Il6Hsa +/-
Ocn +/-; Il6Hsa +/-
ns
Soleus
EDL
Gastrocnemius
Quandricep
C
Soleus
D
NOQ7 Staining
E
Myz2 Staining
F
Type I myofibers (%)
Type II myofibers (%)
G
CSA (μm2)
H
Gene expression relative to Il6f/f (Fold)
myhc-IIa
myhc-IIb
myhc-I
I
Myz2 Staining
NOQ7 Staining
Soleus muscle after endurance
Soleus muscle after endurance

1

2

Figure 4. mIL-6 contributes to the maintenance of muscle mass in an osteocalcin-independent manner

(**A**) Weight of hindlimb muscles of 3-month-old female *Il6$_{Hsa}$-/-* and control littermates, n=6-11. (**B**) Weight of hindlimb muscles in 3-month-old compound mutant mice Osteocalcin+/-;*Il6$_{Hsa}$+/-* and control littermates (control group includes WT, and *Osteocalcin+/-, Il6$_{Hsa}$+/-* mice),n=5-7. (**C**) Representative H&E staining of soleus muscle fibers in 3-month-old female *Il6$_{Hsa}$-/-* and control littermates. Scale bar, 100 μm. (**D-E**) Representative histology with (**D**) N0Q7 (MHC I slow twitch fibers), (**E**) MY32 (MHC II fast twitch fibers) staining of soleus muscle of 3-month-old female *Il6$_{Hsa}$-/-* and control littermates, Scale bar, 100 μm. (**F**) Distribution of type 1 and type II myofibers in 3-month-old female *Il6$_{Hsa}$-/-* and control littermates. Scale bar, 100 μm. (**G**) Measurement of cross section area (CSA) of muscle fibers in 3-month-old female *Il6$_{Hsa}$-/-* and control littermates. (**H**) Expression of myosin heavy chain genes in gastrocnemius muscle measured by qRT-PCR. (**I)** Representative histology with N0Q7 and MY32 staining of soleus muscle after endurance exercise in 3-month-old female *Il6$_{Hsa}$-/-* and control littermates, Scale bar, 100 μm. These experiments are representative of 3 independent experiments. Data shown in A, F, and G, were analyzed by 2-tailed unpaired t test and data in B and H by one-way ANOVA followed by Tukey's post hoc test. Data are represented as mean± SEM, ***P* <0.05.

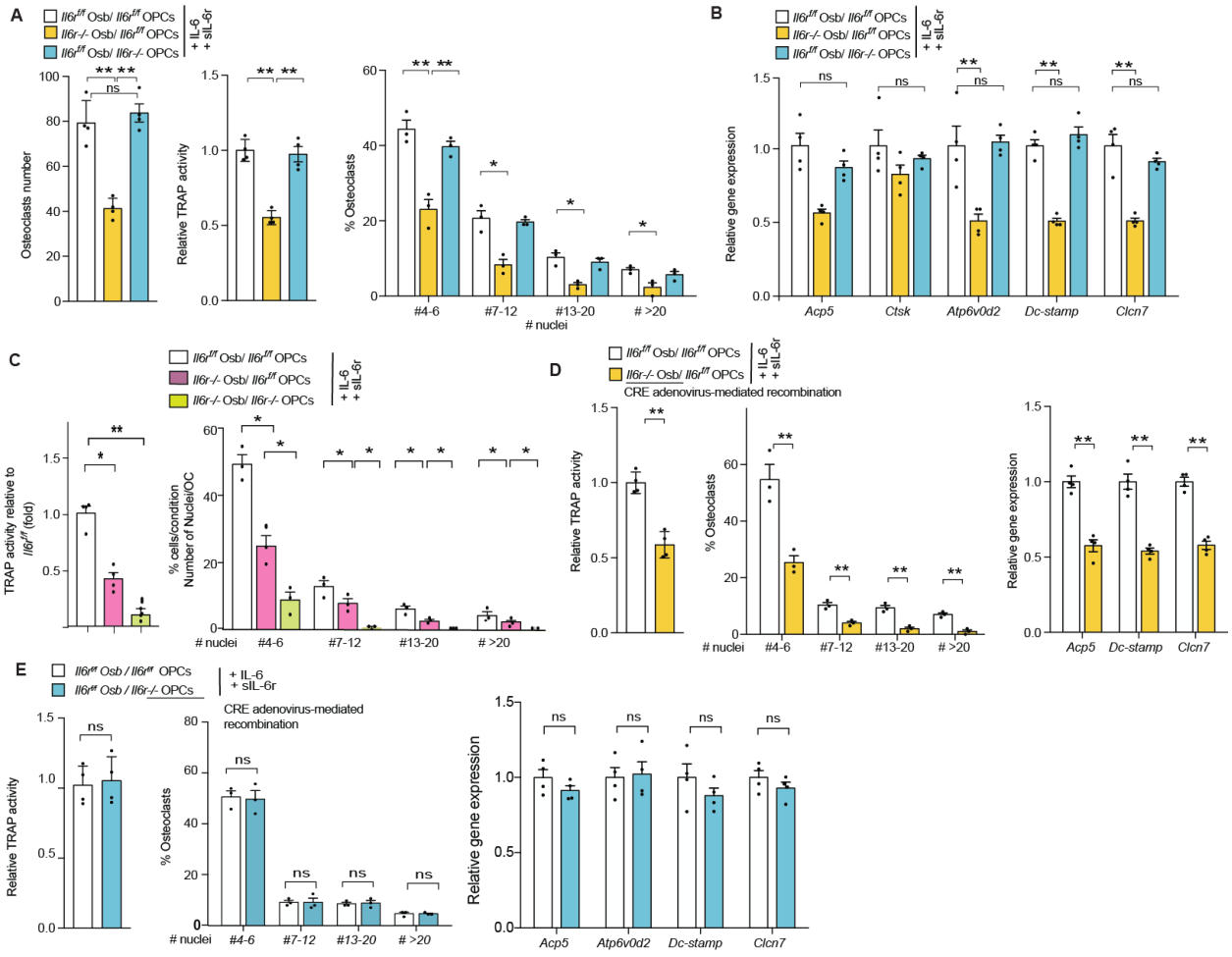
A
Il6r f/f Osb/ Il6r f/f OPCs
Il6r -/- Osb/ Il6r f/f OPCs
Il6r f/f Osb/ Il6r -/- OPCs
+ IL-6 + sIL-6r
Osteoclasts number
Relative TRAP activity
% Osteoclasts
# nuclei
#4-6
#7-12
#13-20
>20
B
Relative gene expression
Acp5
Ctsk
Atp6v0d2
Dc-stamp
Clcn7
C
TRAP activity relative to Il6r f/f (fold)
% cells/condition Number of Nuclei/OC
D
CRE adenovirus-mediated recombination
Relative TRAP activity
% Osteoclasts
Relative gene expression
E
Il6r ff Osb / Il6r ff OPCs
Il6r ff Osb / Il6r -/- OPCs
+ IL-6 + sIL-6r
CRE adenovirus-mediated recombination
Relative TRAP activity
% Osteoclasts
Relative gene expression
ns

Figure 5. IL-6 favors osteoclastogenesis by signaling in osteoblasts

(**A-B**) Co-culture of *Il6r*$^{f/f}$ osteoblasts with *Il6r*$^{f/f}$ osteoclast precursor cells (OPCs), *Il6r*$_{osb}$*-/-* osteoblasts with *Il6*$^{f/f}$ OPCs and *Il6r*$^{f/f}$ osteoblasts with *Il6r*$_{osb}$*-/-* OPCs in presence of IL-6 and and sIL-6r (**A**) Quantification of the number of osteoclasts (OCs), TRAP activity and the number of nuclei per TRAP+ osteoclast. (**B**) Expression of resorbing activity markers *Ctsk, Cathepsin K, Clcn7, Acp5* in mouse osteoclasts (WT OCs). (**C**) Co-culture in the presence of IL-6 and sIL-6r of (1) *Il6r*$^{f/f}$ osteoblasts with *Il6r*$^{f/f}$ OPCs, (2) *Il6r*$_{osb}$*-/-* osteoblasts with *Il6*$^{f/f}$ OPCs, (3) or *Il6r-/-* osteoblasts with *Il6r*$_{osb}$*-/-* OPCs. TRAP activity and quantification of the number of osteoclasts. (**D-E**) *IL6r-/-* osteoblasts were generated by infecting *Il6r*$^{f/f}$ osteoblasts with adenovirus expressing *Cre recombinase* and setting up, co-culture with *Il6r*$^{f/f}$ osteoblasts in the absence or presence of IL-6 in the culture medium. Similarly, *IL6r-/-* OPCs were generated by infecting *Il6r*$^{f/f}$ OPCs with adenovirus expressing *Cre recombinase* and setting up co-culture with *Il6r*$^{f/f}$ osteoblasts in absence or presence of IL-6. (**D**) Quantification of TRAP activity, of the number of nuclei per TRAP+ osteoclast and gene expression of resorption markers (*Ctsk,Dc-stamp Clcn7, Acp5*). (**E**) Co-cultures in the presence of IL-6 in the culture medium, quantification of TRAP activity, of the number of nuclei per TRAP+ osteoclast and expression of resorption markers (*Ctsk, Dc-stamp, Clcn7, Acp5*). These experiments are representative of 3 independent experiments with triplicate samples. Data in A, B, C, D and E were analyzed by 2-way ANOVA followed by Tukey's post hoc test. Error bars represent SEM. **P* < 0.05, ***P* < 0.01. The relative TRAP activity data in A, C, D, E were analyzed by 2-tailed unpaired t test.

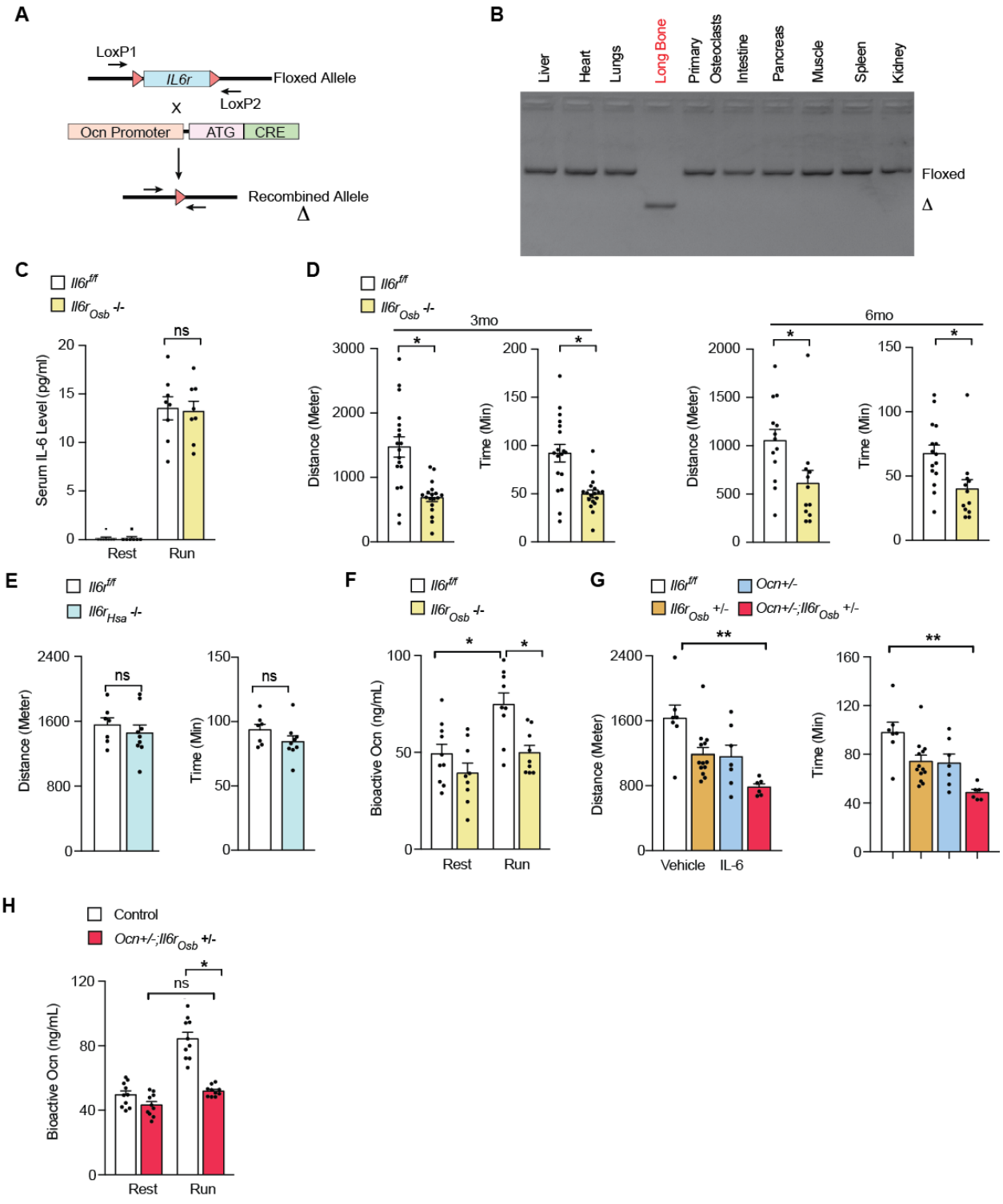
A
LoxP1
IL6r
Floxed Allele
X
LoxP2
Ocn Promoter
ATG
CRE
Recombined Allele
Δ
B
Liver
Heart
Lungs
Long Bone
Primary Osteoclasts
Intestine
Pancreas
Muscle
Spleen
Kidney
Floxed
Δ
C
Il6r f/f
Il6r Osb -/-
Serum IL-6 Level (pg/ml)
ns
Rest
Run
D
Il6r f/f
Il6r Osb -/-
3mo
6mo
Distance (Meter)
Time (Min)
E
Il6r f/f
Il6r Hsa -/-
Distance (Meter)
Time (Min)
ns
F
Il6r f/f
Il6r Osb -/-
Bioactive Ocn (ng/mL)
Rest
Run
G
Il6r f/f
Ocn+/-
Il6r Osb +/-
Ocn+/-;Il6r Osb +/-
Distance (Meter)
Time (Min)
Vehicle
IL-6
H
Control
Ocn+/-;Il6r Osb +/-
Bioactive Ocn (ng/mL)
ns
Rest
Run

Figure 6: IL-6 signaling in osteoblasts is needed to enhance exercise capacity during endurance exercise.

A) Crossing of *Il6r*$^{f/f}$ mice with *Osteocalcin-Cre* mice to delete *Il6r* in differentiated osteoblasts after birth and generate *Il6r*$_{Osb}$*-/-* mice. *Il6r*$_{Osb}$*-/-* mice. **(B**) Detection of *Il6r* deletion by PCR on genomic DNA isolated from in various tissues of *Il6r*$_{Osb}$*-/-* mice. **(C)** Circulating IL-6 levels in 3-month-old *Il6r*$^{f/f}$ and *Il6r*$_{Osb}$*-/-* mice before and after exercise, n=8. (**D**) Performance during an endurance run of 3, and 6-month-old *Il6r*$^{f/f}$ and *Il6r*$_{Osb}$*-/-* mice, n=12-18. (**E**) Performance during an endurance run of 3-month-old *Il6r*$^{f/f}$ and *Il6r*$_{Hsa}$*-/-* mice, n=7-9. (**F**) Circulating Ocn levels at rest and after exercise in bones of 3-month-old *Il6r*$^{f/f}$ and *Il6r*$_{Osb}$*-/-* mice, n=9-10. (**G**) Performance during an endurance run of 3-month-old control (*Il6r*$_{Osb}$*+/-,Osteocalcin+/-* and WT) and *Osteocalcin+/-; Il6r*$_{Osb}$*+/-* mice, n=7-13. (**H**) Circulating Ocn levels in 3-month-old controls (WT, *Il6r*$_{Osb}$*+/- , Osteocalcin+/-)* and *Osteocalcin+/-; Il6r*$_{Osb}$*+/-* mice at rest and after exercise, n=10 each. These experiments are representative of 4 independent experiments. Data shown were analyzed by one-way ANOVA followed by Tukey's post hoc test. Data represent mean±SEM. ***P* <0.05; ****P* <0.01.

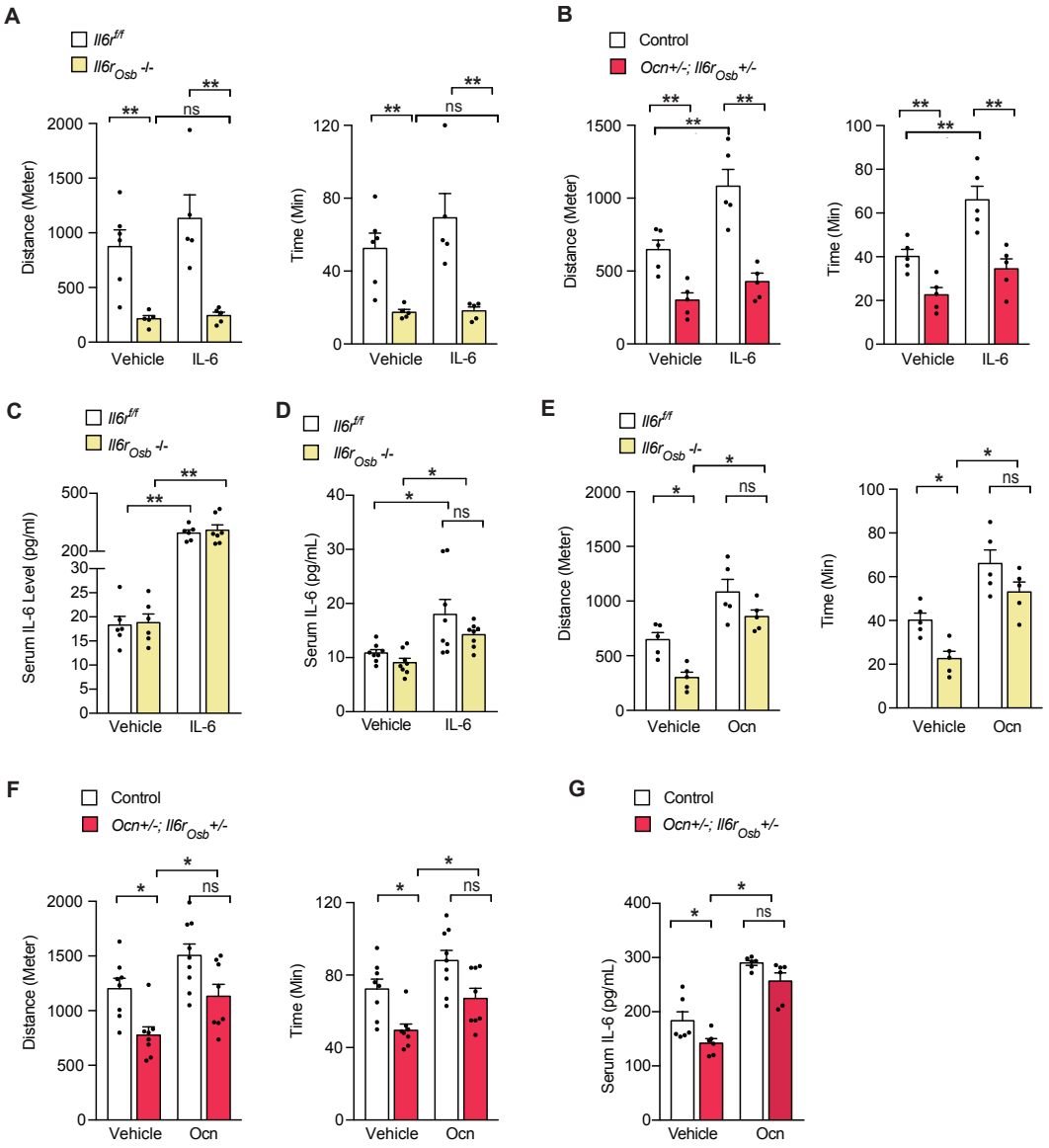
A
Il6r f/f
Il6r Osb -/-
Distance (Meter)
Time (Min)
Vehicle
IL-6
B
Control
Ocn+/-; Il6r Osb +/-
C
Serum IL-6 Level (pg/ml)
D
Serum IL-6 (pg/mL)
E
Ocn
F
G

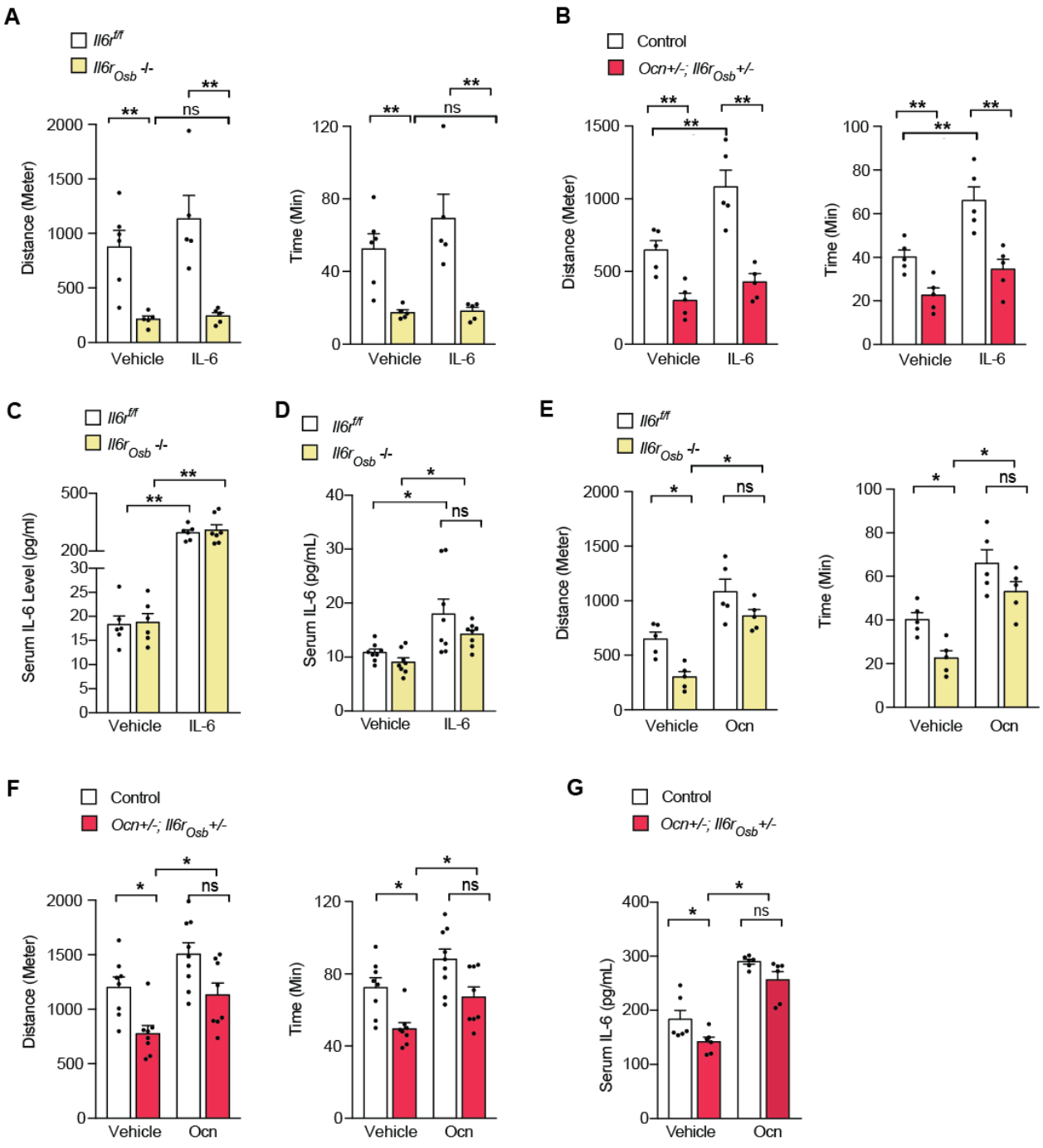
A
Il6r f/f
Il6r Osb -/-
Distance (Meter)
Time (Min)
Vehicle
IL-6
B
Control
Ocn+/-; Il6r Osb +/-
C
Serum IL-6 Level (pg/ml)
D
Serum IL-6 (pg/mL)
E
Ocn
F
G
ns

Figure 7: IL-6 signaling in osteoblasts is needed to enhance exercise capacity during endurance exercise

(A) Performance during an endurance run of 3-month-old *Il6r$^{f/f}$* and *Il6r$_{Osb}$-/-*mice after an i.p. injection of IL-6 (3ng/g), n=6. (**B**) Performance during an endurance run of 3-month-old *Il6r$_{Osb}$+/-;Osteocalcin+/-, Il6r$_{Osb}$+/-, Osteocalcin+/-* and WT mice after an i.p. injection of IL-6 (3ng/g),n=5. **(C)** Circulating levels IL-6 during an endurance exercise in 3-month-old *Il6r$^{f/f}$* and *Il6r$_{Osb}$-/-* mice after i.p. injection of IL-6 (3ng/g), n=6. (**D**) Circulating IL-6 levels in 3-month-old *Il6r$^{f/f}$* and *Il6r$_{Osb}$-/-*mice, n=8 (**E**) Performance during an endurance exercise of 3-month-old *Il6r$^{f/f}$* and *Il6r$_{osb}$-/-*mice treated with osteocalcin (120ng/g), n=5. (**F**) Performance during an endurance exercise of 3-month-old *Il6r$_{Osb}$+/-;Osteocalcin+/-, Il6r$_{Osb}$+/-, Osteocalcin+/-* and WT mice after an i.p. injection of osteocalcin (120ng/g), n=8. (**G**) Circulating IL-6 levels in 3-month-old controls (WT, *Il6r$_{Osb}$+/-, Osteocalcin+/-*) and *Osteocalcin+/-;Il6r$_{Osb}$+/-* mice treated with osteocalcin (120ng/g), n=6. These experiments are representative of 4 independent experiments. Data shown were analyzed by one-way ANOVA followed by Tukey's post hoc test. Results represent the mean± SEM. *P <0.05; **P <0.01.

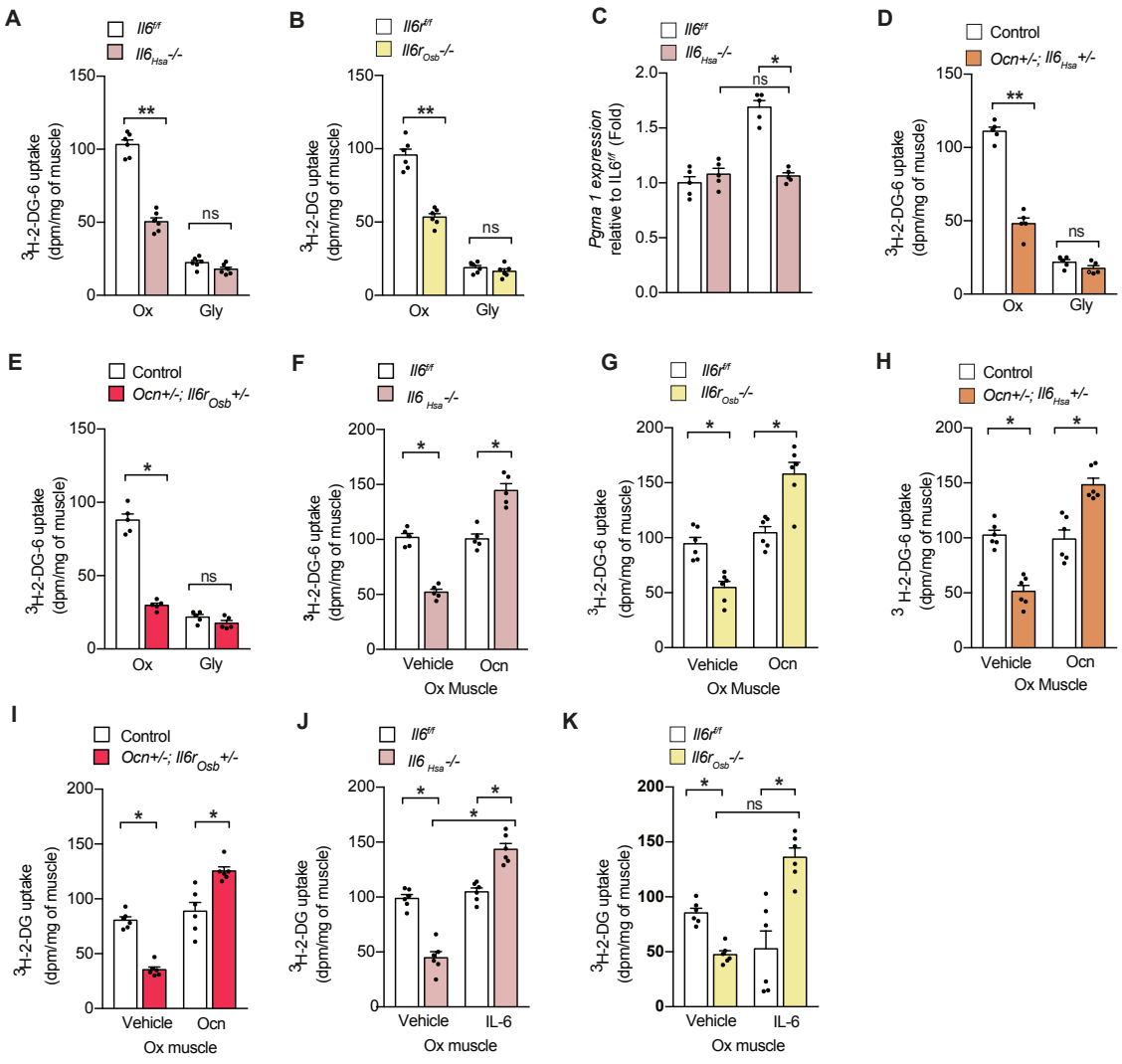
A
Il6f/f
Il6Hsa-/-
3H-2-DG-6 uptake (dpm/mg of muscle)
**
ns
Ox
Gly
B
Il6f/f
Il6rOsb-/-
3H-2-DG uptake (dpm/mg of muscle)
**
ns
Ox
Gly
C
Il6f/f
Il6Hsa-/-
Pgma 1 expression relative to IL6f/f (Fold)
*
ns
D
Control
Ocn+/-; Il6Hsa+/-
3H-2-DG-6 uptake (dpm/mg of muscle)
**
ns
Ox
Gly
E
Control
Ocn+/-; Il6rOsb+/-
3H-2-DG-6 uptake (dpm/mg of muscle)
*
ns
Ox
Gly
F
Il6f/f
Il6 Hsa-/-
3H-2-DG-6 uptake (dpm/mg of muscle)
*
*
Vehicle
Ocn
Ox Muscle
G
Il6rf/f
Il6rOsb-/-
3H-2-DG-6 uptake (dpm/mg of muscle)
*
*
Vehicle
Ocn
Ox Muscle
H
Control
Ocn+/-; Il6Hsa+/-
3 H-2-DG-6 uptake (dpm/mg of muscle)
*
*
Vehicle
Ocn
Ox Muscle
I
Control
Ocn+/-; Il6rOsb+/-
3H-2-DG uptake (dpm/mg of muscle)
*
*
Vehicle
Ocn
Ox muscle
J
Il6f/f
Il6 Hsa-/-
3H-2-DG uptake (dpm/mg of muscle)
*
*
*
Vehicle
IL-6
Ox muscle
K
Il6rf/f
Il6rOsb-/-
3H-2-DG uptake (dpm/mg of muscle)
*
*
ns
Vehicle
IL-6
Ox muscle

1

Figure 8: mIL-6 favors glucose uptake and catabolism in myofibers during exercise through osteocalcin.

(**A**-**B**) Uptake of ^{3}H-2-DG in glycolytic (Gly, white quadriceps) and oxidative (Ox, red quadriceps) muscle in 3-month-old mice **(A)** *Il6$^{f/f}$* vs *Il6$_{Hsa}$*-/- and **(B)** *Il6r$^{f/f}$* vs *Il6r$_{Osb}$-/-* mice after exercise, n=6. (**C**) *Pgma1* expression at rest and after exercise in gastrocnemius muscle of 3-month-old *Il6$^{f/f}$* vs *Il6$_{Hsa}$*-/- mice, n=5 (replicate 3 for each mice). (**D-E**) Uptake of ^{3}H-2-DG in oxidative (Ox, red quadriceps) muscle in 3-month-old (**D**) controls, *Il6$_{Hsa}$*+/- and *Osteocalcin*+/- vs *Osteocalcin+/-; Il6$_{Hsa}$*+/- **(E)** controls (WT, *Il6r$_{Osb}$*+/- and *Osteocalcin*+/-) vs *Osteocalcin+/-; Il6r$_{Osb}$*+/- mice, n=6**.** (**F-I**) Uptake of ^{3}H-2-DG in oxidative (Ox, red quadriceps) muscle after exercise in 3-month-old (**F**) *Il6$^{f/f}$* vs *Il6$_{Hsa}$*-/- **(G)** *Il6r$^{f/f}$* vs *Il6r$_{Osb}$-/-* (**H**) controls (WT, *Il6$_{Hsa}$*+/- and *Osteocalcin*+/-) vs *Osteocalcin+/-;Il6$_{Hsa}$*+/- (**I)** controls (WT, *Il6r$_{Osb}$*+/- and *Osteocalcin* +/-) vs *Osteocalcin+/; Il6r$_{Osb}$*+/- mice treated with osteocalcin (120ng/g) i.p. n=6. (**J-K**) Uptake of ^{3}H-2-DG in oxidative (Ox, red quadriceps) muscle after exercise in 3-month-old mice (**J**) *Il6$^{f/f}$* vs *Il6$_{Hsa}$*-/- (**K**) *Il6r$^{f/f}$* vs *Il6r$_{osb}$-/-* mice treated with IL-6 (3ng/g) i.p. n=6. These experiments are representative of 3 independent experiments. Data shown were analyzed by one-way ANOVA followed by Tukey's post hoc test. Results represent the mean± SEM. **P < 0.01, *P < 0.05.

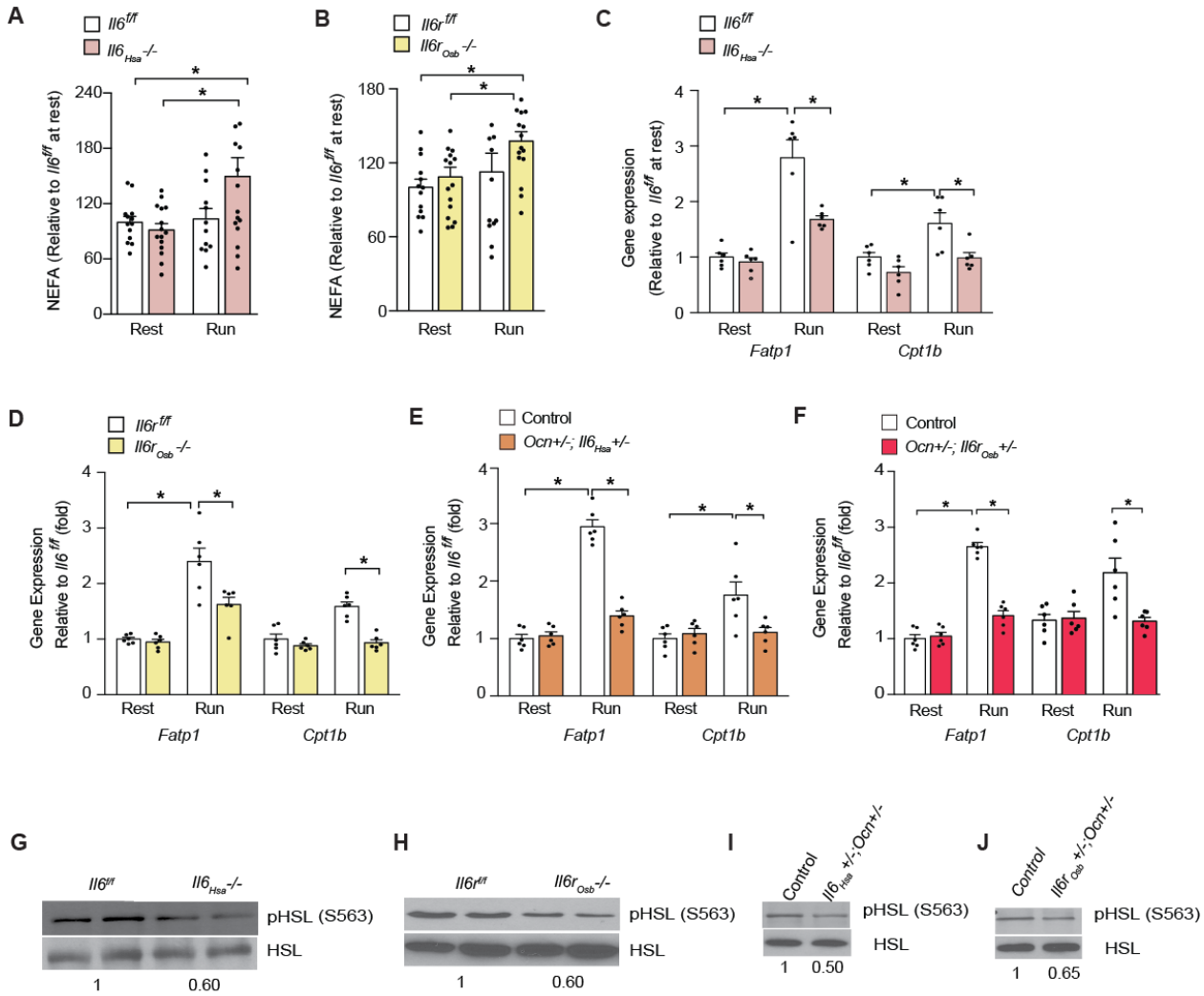
A
Il6f/f
Il6Hsa-/-
NEFA (Relative to Il6f/f at rest)
240
180
120
60
0
Rest
Run
B
Il6rf/f
Il6rOsb-/-
NEFA (Relative to Il6f/f at rest)
180
120
60
0
Rest
Run
C
Il6f/f
Il6Hsa-/-
Gene expression (Relative to Il6f/f at rest)
4
3
2
1
0
Rest
Run
Fatp1
Cpt1b
D
Il6rf/f
Il6rOsb-/-
Gene Expression Relative to Il6f/f (fold)
Fatp1
Cpt1b
E
Control
Ocn+/-; Il6Hsa+/-
Gene Expression Relative to Il6f/f (fold)
Fatp1
Cpt1b
F
Control
Ocn+/-; Il6rOsb+/-
Gene Expression Relative to Il6f/f (fold)
Fatp1
Cpt1b
G
Il6f/f
Il6Hsa-/-
pHSL (S563)
HSL
1
0.60
H
Il6rf/f
Il6rOsb-/-
pHSL (S563)
HSL
1
0.60
I
Control
Il6Hsa+/-;Ocn+/-
pHSL (S563)
HSL
1
0.50
J
Control
Il6rOsb+/-;Ocn+/-
pHSL (S563)
HSL
1
0.65

Figure 9. mIL-6 favors fatty acid uptake and catabolism in myofibers during exercise through osteocalcin.

(**A-B**) Circulating NEFA levels at rest and after exercise in 3-month-old *Il6$_{Hsa}$-/-* and *Il6r$_{Osb}$-/-* mice and their respective controls. (**C-F**) Expression of *Fatp1* and *Cpt1b* at rest and after exercise in gastrocnemius of 3-month-old (**C**) *Il6$^{f/f}$* and *Il6$_{Hsa}$-/-* mice, (**D**) *Il6r$^{f/f}$* vs *Il6r$_{osb}$-/-* mice, (**E**) controls (WT, *Il6$_{Hsa}$*+/- and *Osteocalcin*+/-) vs *Osteocalcin+/-*;*Il6$_{Hsa}$*+/- mice (**F**) controls (WT, *Il6r$_{Osb}$*+/- and *Osteocalcin*+/-) vs *Osteocalcin+/-*;*Il6r$_{Osb}$*+/- mice. (**G-J**) Western blot analysis of HSL phosphorylation (Ser563) in tibialis muscles of 3-month-old (**G**) *Il6$^{f/f}$* vs *Il6$_{Hsa}$-/-,* (**H**) *Il6r$^{f/f}$* vs *Il6r$_{Osb}$-/-*, (**I**) controls (WT, *Il6$_{Hsa}$*+/- and *Osteocalcin* +/-) vs *Osteocalcin +/-*; *Il6$_{Hsa}$*+/- (**J**) controls (WT, *Il6r$_{Osb}$*+/- and *Osteocalcin*+/-) vs *Osteocalcin+/-*;*Il6r$_{Osb}$*+/- mice after exercise. These experiments are representative of 3 independent experiments. Data in A, B, C, D and E were analyzed by 1-way ANOVA followed by Tukey's post hoc test. Error bars represent SEM. Results represent the mean± SEM. *P <0.05; **P <0.01.

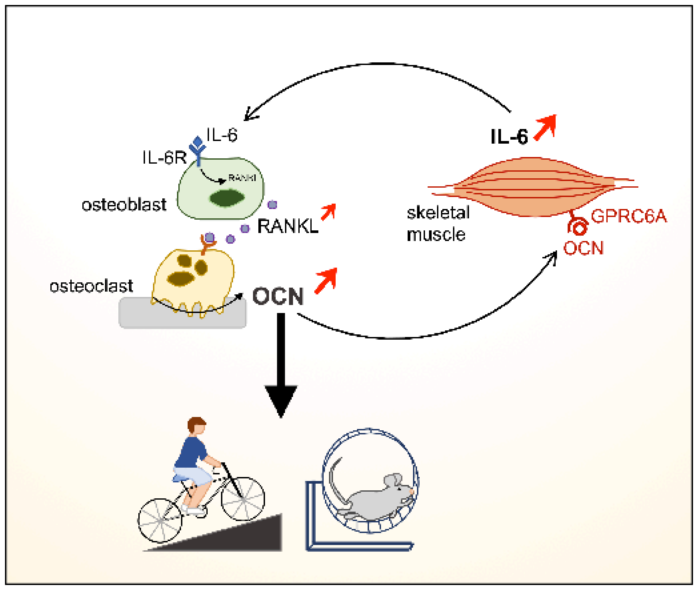

Figure 10: Schematic representation of how muscle derived interleukin 6 increases exercise capacity in an osteocalcin-dependent manner.

Table 1: Summary of effects of intraperitoneal injection of osteocalcin or IL-6 during Endurance run in different mouse strains.

Genotpe	Treatment	Glucose Uptake	Ocn Levels	IL-6 Levels	Run
Il6$_{Hsa}$-/-	Vehicle	Low	↓	↓	↓
	Ocn (120ng/g)	Rescued	↑	↑	↑
	IL-6 (3ng/g)	Rescued	↑	↑	↑
Il6r$_{Osb}$-/-	Vehicle	Low	↓	↓	↓
	Ocn (120ng/g)	Rescued	↑	↑	↑
	IL-6 (3ng/g)	Low	→	↑	↓
Ocn+/-; Il6$_{Hsa}$+/-	Vehicle	Low	↓	↓	↓
	Ocn (120ng/g)	Rescued	↓	↑	↑
	IL-6 (3ng/g)	Rescued	↑	↑	↓
Ocn+/-; Il6r$_{Osb}$+/-	Vehicle	Low	↓	↓	↓
	Ocn (120ng/g)	Rescued	↑	↑	↑
	IL-6 (3ng/g)	Low	→	↑	↓